Frost Depth Analysis Explanation

Prepared by Structural TAG Panelist Mitch Okeson.

7/23/24

Background:

The model building codes reference the ASCE 32-01 Design and Construction of Frost-Protected Shallow Foundations as an accepted standard for adequate frost protection of heated, semi-heated, and unheated buildings. A proposal has been introduced to realign the required frost depth within the State of Minnesota based upon this analytical reference standard to replace the historic State requirements which were based upon more empirical information.

The reference standard methodologies are straightforward with respect to heated buildings. Heated buildings in accordance with the standard are any structure in which the Minimum Average Monthly Indoor Temperature is equal to or greater than 63 degrees Fahrenheit. The commentary of the Standard indicates that "homes, businesses, and other buildings with year-round human occupancy are assumed to have an average monthly indoor air temperature of more than 63 degrees and should be constructed as heated buildings".

The Standard states that "semi-heated buildings or parts of buildings are assumed to have an average monthly indoor air temperature between 41 degrees and 63 degrees Fahrenheit". It further defines that semi-heated spaces "included are unconditioned spaces that receive significant indirect heat from conditioned spaces, such as unfinished basements, unvented crawlspaces, and buildings that are maintained during the winter season with reduced heating". The standard also indicates that "approved attached garage designs may be classified as semi-heated, where heat, provided to the garage by thermal conditioning, or heat loss from the building, maintains a minimum monthly average temperature of 41 degrees Fahrenheit during the design winter".

The Standard states that unheated buildings are those in which the Minimum Average Monthly Indoor Temperature is less than 41 degrees Fahrenheit. It further indicates that "unheated buildings are typically detached storage structures or parts of structures that are unheated and thermally separated from the ancillary heat transfer from conditioned areas of the building".

The Standard states that "minor or temporary variations below the average monthly indoor temperature requirements are not detrimental to the performance of buildings classified as heated or semi-heated for the purposes of FPSF design".

Greg Metz prepared a Code Change Proposal for 1303.1600 which proposed minimum foundation depths for both heated and unheated structures based upon the ASCE 32-01 Standard. Excerpts from that Code Change Proposal will be used herein.

Discussion:

Heated Buildings

The methods of the ASCE 32-01 can be followed to determine the required frost depth for heated structures. This work was completed as depicted in the Code Change Proposal and appears to correctly represent the minimum frost depth based upon the Air Freezing Index methodologies within the Standard for the given AFI F100 values utilized.

Semi-Heated Buildings

The ASCE 32-01 standard states that determination of frost depth of semi-heated heated buildings shall equal the frost depth for heated buildings plus 8" of extra depth. The performance of many attached garages of heated buildings, if built as insulated, could generally be considered semi-heated buildings as the thermal performance within the enclosed space is often above the 41 degrees monthly average. Of course, short term cold snaps occur wherein the average temperature may be lower than 41 degrees, but the standard acknowledges that that will occur. Clearly judgement herein is necessary, but simply because an attached garage, or crawlspace, or similar space is not conditioned does not automatically mean that it is excluded from being considered a semi-heated space.

Unheated Buildings

The ASCE 32-01 states that ground insulation Rg may be reduced by 0.3R for every 1-inch increase in soil cover thickness, above the 10-inch minimum, over the ground insulation. Accordingly, one can calculate the required burial depth of the foundation element whereas the required R-value of the insulation below the footing reduces to zero. The Mean Annual Temperature Table A8 from the ASCE 32-01, shown below for reference, is used to determine the R-value of the ground insulation below the footings.

TABLE A8. Minimum Thermal Resistance (R-Value) of Ground Insulation, R_g, and Horizontal Extension, D_g, for Unheated Buildings

		Mean Annual Temperature (°F):				
F_{100} (°F-days)	D_g (inches)	≤32	36	38	40	≥41
750 or fewer	30	5.7	5.7	5.7	5.7	5.7
1,500	49	13.1	9.7	8.5	8.0	6.8
2,250	63	19.4	15.9	13.6	11.4	10.2
3,000	79	25.0	21.0	18.2	15.3	14.2
3,750	91	31.2	26.1	22.7	—	—
4,500	108	37.5	31.8	—	—	—

Interpolation shall be permitted.

Based upon the tabulated data much of Minnesota's unheated buildings would be categorized in the zone of the table which has the values blanked out. In order to obtain a complete dataset, as well as expand the data set higher than 44 degrees, excel was used to determine the most appropriate trendline equation to calculate the anticipated Rg values to expand the ASCE 32-01 table. Below is a depiction of the expanded trendline graphing as well as the expanded table.

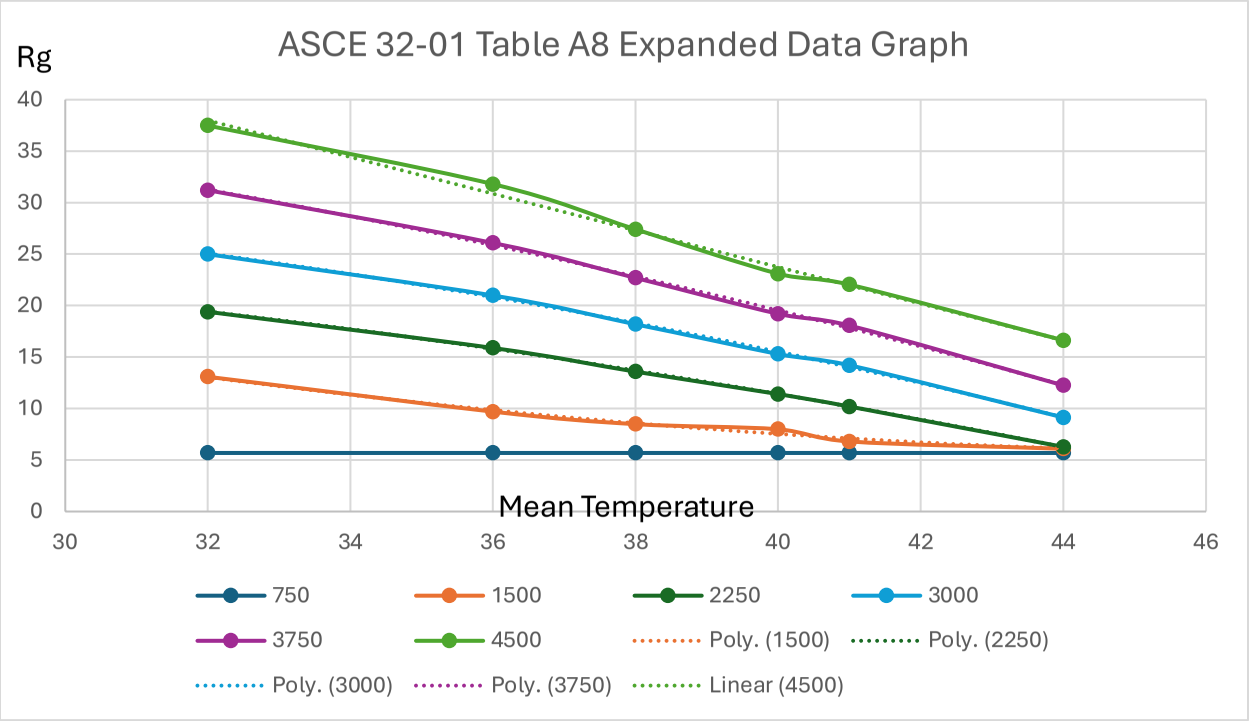

AFI	Mean Annual Temperature					
F100	32	36	38	40	41	44
750	5.7	5.7	5.7	5.7	5.7	5.7
1500	13.1	9.7	8.5	8	6.8	6.1
2250	19.4	15.9	13.6	11.4	10.2	6.3
3000	25	21	18.2	15.3	14.2	9.1
3750	31.2	26.1	22.7	19.2	18.1	12.3
4500	37.5	31.8	27.4	23.1	22.1	16.6

Further expanding this table to add the 3,500 & 4,000 AFI F100 values for easy reference.

AFI	Mean Annual Temperature					
F100	32	36	38	40	41	44
750	5.7	5.7	5.7	5.7	5.7	5.7
1500	13.1	9.7	8.5	8	6.8	6.1
2250	19.4	15.9	13.6	11.4	10.2	6.3
3000	25	21	18.2	15.3	14.2	9.1
3500	29.1	24.4	21.2	17.9	16.8	11.2
3750	31.2	26.1	22.7	19.2	18.1	12.3
4000	33.3	28.0	24.3	20.5	19.4	13.7
4500	37.5	31.8	27.4	23.1	22.1	16.6

Figure A2 from the ASCE 32-01 depicts the Mean Annual Temperature.

FIGURE A2, Continued. Mean Annual Temperature (°F) Contour Map For The United States.

The Mean Annual Temperature data suggests that the average value for Minnesota would be approximately 40.0 degrees. To get a better estimate of this Mean Average Temperature the NOAA Climate at a Glance County Mapping online service was utilized to obtain the Mean Average

Temperature for each County in Minnesota. This data provides the average annual mean temperature measured from 1901-2000.

https://www.ncei.noaa.gov/access/monitoring/climate-at-a-glance/county/mapping/21/tavg/202406/60/value

Using this data the average Mean Annual Temperature for each county was utilized to calculate an average for the three state zones suggested by the Code Change Proposal. The county separation line proposed in the Code Change Proposal appears to accurately follow the ASCE 32-01 Air Index contours. However, three counties within the state have large gradients across their broad size: Cook, Lake, and St. Louis. Much of these counties' land mass is unpopulated with most of the population occurring along the North Shore. The average annual mean temperature for the land mass does not seem to accurately reflect the average mean temperature for the areas of populus. For the purposes of determining the average mean temperature for each of the zones it seems that the data for those three counties respectively should be used for the Zone 3 area and neglected for the Zone 2 area. Those three counties mean annual temperature is significantly less than the other Zone 2 counties and even less than most of the Zone 3 counties.

Utilizing the NOAA annual mean temperature and the expanded ASCE 32-01 Table A8 generated the following results are determined for each zone.

Zone I - Mean Annual Temperature

County	1901 - 2000 Mean
Big Stone	42.4
Lac qui Parle	43.2
Yellow Medicine	43.6
Lincoln	42.7
Pipestone	43.1
Rock	44.2
Lyon	43.7
Murray	43.2
Nobles	43.8
Swift	42.2
Chippewa	43.0
Stearns	41.2
Kandiyohi	42.1
Renville	43.5
Redwood	44.0
Brown	44.3
Cottonwood	43.7
Jackson	43.9
Watonwan	44.4
Martin	44.3
Meeker	42.2
Mcleod	43.2
Sibley	43.9
Nicollet	44.4
Blue Earth	44.6
Faribault	44.7
Benton	41.2
Mille Lacs	40.5
Kanabec	40.5
Pine	39.7
Sherburne	42.1
Isanti	42.1
Chisago	42.4
Anoka	43.0
Wright	42.5
Hennipen	43.5
Ramsey	43.8
Washington	43.6
Carver	43.6
Scott	44.1
Dakota	44.1
Le Sueur	44.1
Rice	43.7
Goodhue	43.6
Waseca	43.9
Steele	43.4
Dodge	42.9
Olmsted	43.2
Wabasha	43.9
Winona	44.0
Freeborn	43.9
Mower	43.1
Fillmore	43.6
Houston	44.8
Average	43.2
ASCE 32-01 F100:	3,000
ASCE 32-01 Table A8	10.46
ASCE 7.1 Step 3	
0.3 R per In Cover over 10"	35
10" Min Cover	10
Total Depth, inches	45
Proposed Heated Frost Depth, inches	32
Increase for Unheated, inches	13

Zone II - Mean Annual Temperature

County	1901 - 2000 Mean
Clay	40.1
Wilkin	41.0
Traverse	41.9
Ottertail	39.8
Grant	41.0
Douglas	40.1
Stevens	41.6
Pope	40.9
Hubbard	38.3
Wadena	39.3
Todd	40.0
Cass	38.6
Crow Wing	39.5
Morrison	40.5
Aitkin	38.5
Carlton	38.2
Average	40.0
ASCE 32-01 F100:	3,500
ASCE 32-01 Table A8	17.9
ASCE 7.1 Step 3	
0.3 R per In Cover over 10"	60
10" Min Cover	10
Total Depth, inches	70
Proposed Heated Frost Depth, inches	44
Increase for Unheated, inches	26

Zone III - Mean Annual Temperature

County	1901 - 2000 Mean
Kittson	36.7
Roseau	36.1
Marshall	37.4
Lake of the Woods	36.1
Koochiching	36.4
Beltrami	37.1
Polk	38.7
Pennington	37.8
Red Lake	38.3
Clearwater	37.6
Norman	39.5
Mahnomen	38.2
Itasca	37.2
St Louis	36.4
Lake	35.9
Cook	35.2
Becker	38.7
Average	37.3
ASCE 32-01 F100:	4,000
ASCE 32-01 Table A8	25.6
ASCE 7.1 Step 3	
0.3 R per In Cover over 10"	85
10" Min Cover	10
Total Depth, inches	95
Proposed Heated Frost Depth, inches	60
Increase for Unheated, inches	35

The results of utilizing the ASCE 32-01 methodologies calculate an approximate foundation depth for unheated buildings as follows:

Zone 1 = 1.0 feet extra
Zone 2 = 2.0 feet extra
Zone 3 = 3.0 feet extra

Averaging these values would yield a 2.0 feet extra burial depth for unheated buildings over which would be required for heated buildings.

Heated Buildings – Further Analysis

The heated building analysis provided utilized an AFI F100 value of 3,000, 3,500, and 4,000 for the three zones. These values each represent the highest value within the proposed zone. The results are di erent if we used the average value within the proposed zones.

- Zone 1 – Under 3,000
  - Assume Average AFI is 2,750
  - From Table A5: Foundation Depth at Corner w/o Wing Insulation = 27”
  - Foundation Depth for “Semi-Heated” would be approximately = 35”
- Zone 2 – Under 3,500 but Above 3,000
  - Assume Average AFI is 3,250
  - From Table A5: Foundation Depth at Corner w/o Wing Insulation = 37”
  - Foundation Depth for “Semi-Heated” would be approximately = 45”
- Zone 3 – Above 3,500
  - Assume Average AFI is 3,850
  - From Table A5: Foundation Depth at Corner w/o Wing Insulation = 54”
  - Foundation Depth for “Semi-Heated” would be approximately = 62”

The “average” foundation depth required in the respective zone is less than right at the edge of the zone. Adding the ASCE 32-01 required extra 8” of depth for semi-heated places the average zone depth similar to the depth at the upper end of the zone northern border.

Summary of Analysis:

The ASCE 32-01 methodologies were followed by utilizing a more extensive temperature database as well as mathematically extrapolating the unheated ground insulation table. From this analysis the Standard would provide the following foundation depths for the Code Change Proposal zones.

Zone 1

Heated – Buildings conditioned to above 63 degrees = 2’-8”
Semi-Heated – Buildings conditioned to between 41 & 63 degrees = 3’-4”

Unheated – Buildings conditioned to below 41 degrees = 3’-9”

Zone 2

Heated – Buildings conditioned to above 63 degrees = 3’-8”
Semi-Heated – Buildings conditioned to between 41 & 63 degrees = 4’-4”
Unheated – Buildings conditioned to below 41 degrees = 5’-10”

Zone 3

Heated – Buildings conditioned to above 63 degrees = 5’-0”
Semi-Heated – Buildings conditioned to between 41 & 63 degrees = 5’-8”
Unheated – Buildings conditioned to below 41 degrees = 7’-11”

Opinion of Author:

The State of Minnesota has specified a foundation depth for all structures for many years. To my knowledge and the knowledge of other structural engineer colleagues; frost heave of foundation elements has not been an issue which arises often. Frost heaving of slabs on grade, shallow thickened edge slabs, or similar construction has been observed; however, that is to be expected as that construction did not comply with the required frost depth. Accordingly, if we as design professionals are not seeing frost depth failures of heated, semi-heated, or unheated buildings with frost depth foundations meeting the current requirements of the State of Minnesota then I am hesitant to increase the foundation depth required.

In my opinion I support the use of the ASCE 32-01 usage to determine the required foundation depths of heated and semi-heated buildings. I do not support the use of the ASCE 32-01 for mandating a minimum foundation depth for unheated structures by the State of Minnesota.

Per the ASCE 32-01 unheated buildings are those which are not occupied by humans. Accordingly, these unheated buildings are nearly always utility/storage type facilities wherein I believe that the Owner of said buildings should be able to elect the degree of frost protection beyond the minimum required for heated buildings that they believe is su icient to protect their investment. Furthermore, the ASCE 32-01 states specifically:

> “The design provisions in the Standard are based on the following worst-case conditions to ensure adequate frost protection:
>
> - Use of a 100-year mean return period air-freezing index
> - A highly frost-susceptible soil (silt) with relatively high thermal conductivity and with su icient moisture in the soil to promote frost heave, but not so much as to resist the penetration of the frost line through latent heat e ects
> - No insulating ground cover from snow, turf, and so on

- Minimum indoor temperature conditions for “heated” and “semi-heated” building thermal classifications
- No heat input to the ground from buildings classified as “unheated”

Several of these conditions would need to be violated simultaneously for frost heave to occur on a site that actually had frost-susceptible soils of su iciently high moisture content. Thus, frost heave is highly improbable for buildings with foundations properly designed using the FPSF technology. The rare reported problems have typically been associated with designs or construction that are not in compliance with good design and construction practices.”

The Standard clearly states that it is providing a worst-case scenario design, which clearly is not a minimum design standard. I do not think it is appropriate for the State of Minnesota to mandate the minimum standard of care to the degree of the most extreme worst-case scenario possible.

In my opinion I believe that the State of Minnesota should specify an appropriate minimum frost depth for conditioned buildings and then let Owners and/or Design Professionals determine what methods are appropriate for addressing frost heave risk on unconditioned buildings.

I support a three Zone system which specifies a required frost depth for conditioned buildings at 3.0 feet, 4.0 feet, and 5.0 feet. I assume that conditioned buildings are all those which meet the ASCE 32-01 definition for “heated” and “semi-heated”; thus, any building which is maintained above 41 degrees average monthly indoor temperature. As indicated in the “*Heated Buildings – Further Analysis”* section above, the average frost depth for semi-heated buildings in the proposed zones is at the proposed depths that I suggested.

Development of Frost Depth Maps for the United States

Prepared for

U.S. Department of Housing and Urban Development
Office of Policy Development and Research
Washington, DC

Contract No. H-21172CA

and

National Association of Home Builders
Program for Research and Optimum Value Engineering (PROVE)
Washington, DC

by

NAHB Research Center, Inc.
Upper Marlboro, Maryland

July 2001

NOTICE

The work that provided the basis for this publication was supported by funding under a grant with the U.S. Department of Housing and Urban Development. The substance and findings of the work are dedicated to the public. The author is solely responsible for the accuracy of the statements and interpretations contained in this publication. Such interpretations do not necessarily reflect the views of the Government.

ABOUT THE NAHB RESEARCH CENTER, INC.

The NAHB Research Center is a not-for-profit subsidiary of the National Association of Home Builders (NAHB). The NAHB has 200,000 members, including 50,000 builders who build more than 80 percent of new American homes. NAHB Research Center conducts research, analysis, and demonstration programs in all areas relating to home building and carries out extensive programs of information dissemination and interchange among members of the industry and between the industry and the public.

EXECUTIVE SUMMARY

This document is a compilation of two phases of research resulting in the development of frost depth (penetration) maps for use in the United States for building foundation design and other applications. The work was conducted at the Northeast Regional Climate Center of the National Oceanic and Atmospheric Administration (NOAA) located at Cornell University, Ithaca, New York.

In the first phase of work, an existing simulation model was modified and validated to realistically predict frost penetration into ground under variable soil and climatic conditions found in the United States. The simulation model was modified to incorporate a water budgeting scheme (soil moisture content) and an alteration of the equation for soil thermal conductivity. Using only daily temperature, liquid precipitation, snowfall, and snow cover, the new model allowed the simulation of maximum seasonal frost depths across the United States. Observed soil freezing depths, ranging from 0 to over 100 cm (39.4 inches), were simulated with an average absolute error of 5.4 cm (2.1 inches). Thus, the model was found to be very accurate in the prediction of frost penetration depths in the United States. The report on the model's development and validation, which supports the second phase of work, is included in Appendix A of this document.

In the second phase of work, the simulation model was used to develop extreme-value statistics (return period estimates) for frost penetration depths in the United States. To evaluate extreme-value statistics, the model was run using daily temperature data, snow depth data, and precipitation data from a set of 3000 U.S. cooperative weather stations for the corresponding year of record. Each run produced an annual-extreme frost depth estimate. The simulated data was subsequently analyzed with respect to identifying the appropriate extreme-value statistical distribution. The main body of this document reports on the second phase effort.

To complete the second phase effort, frost penetration maps for various return periods (2-, 5-, 10-, 25-, 50-, and 100-year) were developed based on maximum annual frost depth under bare soil and sod using observed snow cover conditions. Maps were also generated for snow-free bare soil conditions. The maps are found in Appendix B of this document. In addition, the sensitivity of mapped frost depths to soil characteristics (i.e., porosity, moisture content, and clay content) was investigated; adjustment factors to account for variation in soil characteristics were developed.

Future activities are needed to develop a single design frost depth map for building foundation construction in the United States. The map development should consider the frost depth maps in Appendix B as well as currently accepted local practice in the United States. Frost depths used for building foundation design (i.e., specification of footing depth) and protection of utilities (e.g., under-ground water pipes) against freezing are based on local experience. While this practice has been generally successful, it can result in great differences in local practice, even within similar climates and soil conditions. Thus, it is anticipated that a newer map based on this document could bring greater uniformity and risk-consistency to the specification of frost depths in the United States for efficient building construction and other relevant applications.

TABLE OF CONTENTS

Extreme-Value Statistics for Frost Penetration Depths in the United States

Final Report

Prepared for

NAHB Research Center, Inc.
Cooperative Agreement

by

Arthur T. DeGaetano
and
Daniel S. Wilks
Northeast Regional Climate Center
Cornell University
Ithaca, NY 14853

December 2000

INTRODUCTION

Extreme values of the maximum depth of soil freezing are of interest for engineering design specifications. For instance, building codes must consider the maximum depth of frost penetration to assure that footings and utilities are buried at the appropriate depths. If these specifications are too lax, freezing conditions are likely to result in structural damage during the design lifetime of the structure. Alternatively, codes that are too stringent inflate building costs unnecessarily due to increases in labor and material costs. Unfortunately, the only direct practical analysis of maximum soil freezing depths in the U.S. is based on unofficial, undocumented and antiquated (1899-1938) measurements (USDA 1941). More recently, Crandell et al. (1994) present a map of 100-year return period air freezing indices which can be used to derive empirical frost depth values. However, these values neglect the effects of a changing winter snow cover.

Due to the lack of relevant climatological data, building codes concerned with soil freezing levels are often subjectively developed based on intuition, undocumented observations, and unrepresentative ground surface conditions. Although national building codes, such as those published by Building Officials and Code Administrators International (BOCA) give detailed specifications for such climate-dependent building codes as roof snow loads and wind stress, the recommendation for footing depth is simply "below the local frost line". The National Building Code of Canada is equally vague in its recommendation that footing depths be determined based on local experience. As a result, building codes often vary considerably across political boundaries. For instance, across the New York–Vermont border local building codes for footing depths range from 183 cm in Williston, VT to 121 cm in Plattsburgh, NY, 47 km to the west.

This disparity in regional building codes and the paucity of measured frost depth and soil temperature data led us to develop a one-dimensional heat flow model capable of estimating frost depths using only meteorological variables measured at cooperative network weather stations (DeGaetano et al., 1996). This U.S. National Weather Service network is composed of volunteer observers who report daily values of temperature, precipitation and snow depth. Since historical data from these sites extend from the late nineteenth century to the present, and given that approximately 8000 stations are in operation nationwide model-derived frost depths can be developed having a relatively high spatial resolution. These values can then be used to produce an extreme-value analysis for the maximum depth of soil freezing having this same resolution.

DESCRIPTION OF MODEL

A complete description of the model development and testing phases of this research is given in the manuscript "Physical Simulation of Maximum Seasonal Soil Freezing Depth in the United States using Routine Weather Observations". A copy of this paper, which will be published in the *Journal of Applied Meteorology* in early 2001, is included in Appendix A.

EXTREME-VALUE ANALYSIS

The magnitudes of extreme soil freezing events corresponding to average return periods longer than the climatic record (i.e., with exceedence probabilities smaller than the reciprocal of the

length of record) must be extrapolated beyond the observed data. A convenient and consistent approach to this extrapolation is to fit an appropriate probability distribution to the annual maximum data, and then evaluate quantiles of that fitted distribution corresponding to the desired exceedence probabilities. Although this approach has been used for a variety of meteorological parameters such as rainfall (Wilks, 1993), snow depth (Schmidlin et al., 1992), snowpack water equivalent (Wilks and McKay, 1996), wind (Simiu et al., 1982) and air freezing index (Crandell et al., 1994) a rigorous statistical analysis of soil freezing depth extremes is lacking.

A suite of candidate distributions was screened for possible use in representing annual extreme soil freezing depth values generated by the model. The beta-P, beta-κ, generalized gamma, generalized extreme-value (GEV), generalized Pareto, trans-normal, 3-parameter lognormal, Gumbel and Revfiem distributions (all described in Wilks 1993) were fit using the method of maximum likelihood. These are three-parameter distributions with the exception of the Gumbel which has only two parameters. In addition, the 4-parameter kappa distribution (Hosking and Wallace 1993) and the 5-parameter Wakeby distribution (Houghton 1978) were fit using the L-moment algorithms of Hosking (1991). Separate Gumbel, GEV and generalized Pareto distributions were also fit using these L-moment algorithms.

Since the performance of these distributions on the extreme right tail is of primary interest in extreme-value analysis, conventional goodness-of-fit measures are of little help in distinguishing the most appropriate probability model. An alternative approach, using a bootstrap procedure described by Wilks (1993) is therefore employed here. Model-derived maximum frost depths were obtained for a geographically representative set of 17 cooperative observer network stations. The selected stations were required to have at least 50 years of meteorological observations with minimal missing data. Serially complete temperature records for the 1951-93 period were available at each site (DeGaetano et. al, 1995). Prior and subsequent to this period, data from adjacent stations were used as estimates for missing temperature observations during October through April. In a limited number of cases where data from adjacent stations was also unavailable, missing temperatures were estimated based on the previous and subsequent daily temperature value. From April through October missing temperatures were set to the 30–year average daily temperature (for the purpose of defining the annual course of the "deep" temperature). Stations were also required to have minimal missing snow depth data. Since sites without missing snow depth observations were uncommon, it was necessary to estimate these values in some instances. In these cases, either the most recent available snow depth observation or data from an adjacent station was used as a surrogate for the missing observation. Missing precipitation and snowfall measurements were less common and are not as problematic in the model. Therefore these values were either replaced or inferred with data from an adjacent site, or prior and/or subsequent days. Years in which any missing data values occurred for more than 14 sequential days during October through April were not considered. In all cases, the meteorological data were required to pass the quality-control procedure of Robinson (1993).

Once the series of maximum annual frost depths was constructed for a station, random samples of size 30 were repeatedly (1000 times) drawn from these records, with replacement. Each of these 1000 samples was then used to fit each of the candidate distributions. Extrapolations to data values corresponding to the exceedence probabilities of the largest points in the parent data set were then made according to each of the 1000 parameter sets for each candidate distribution.

This procedure simulates the extrapolations to unknown extreme frost depths that are to be required, and yields information on the bias and precision of these extrapolations.

Figure 1 illustrates bootstrap results for the largest modeled annual maximum frost depth at 3 climatically diverse sites, Fredonia, New York; Langley, Virginia; and Caribou, Maine. Sample sizes at these stations are 67, 59 and 57 years, respectively, which correspond to exceedence probabilities of 0.0147 at Fredonia 0.0167 at Langley and 0.0172 at Caribou. Each boxplot represents the distribution of 1000 extrapolations to the maximum annual frost depth specified by the appropriate exceedence probability. Whiskers are located at the 5th and 95th percentiles. The boxplots for the candidate extreme value distributions using Fredonia (Fig. 1a) data are arranged in decreasing order of the medians of their respective bootstrapped extrapolations. Bootstrap results vary somewhat from station to station, but those shown in Fig. 1 are representative of the 17 sites, particularly in that no geographic biases were evident among the analyses. Boxplots for the Gumbel, GEV and generalized Pareto distributions fit using L-moments were nearly identical to those derived from the maximum likelihood fitting of these distributions and therefore are excluded from Figure 1. In addition the boxplot for the 3-parameter lognormal is omitted due to the gross overestimates of the target frost depths and excessive sampling dispersion which characterized this distribution at all stations.

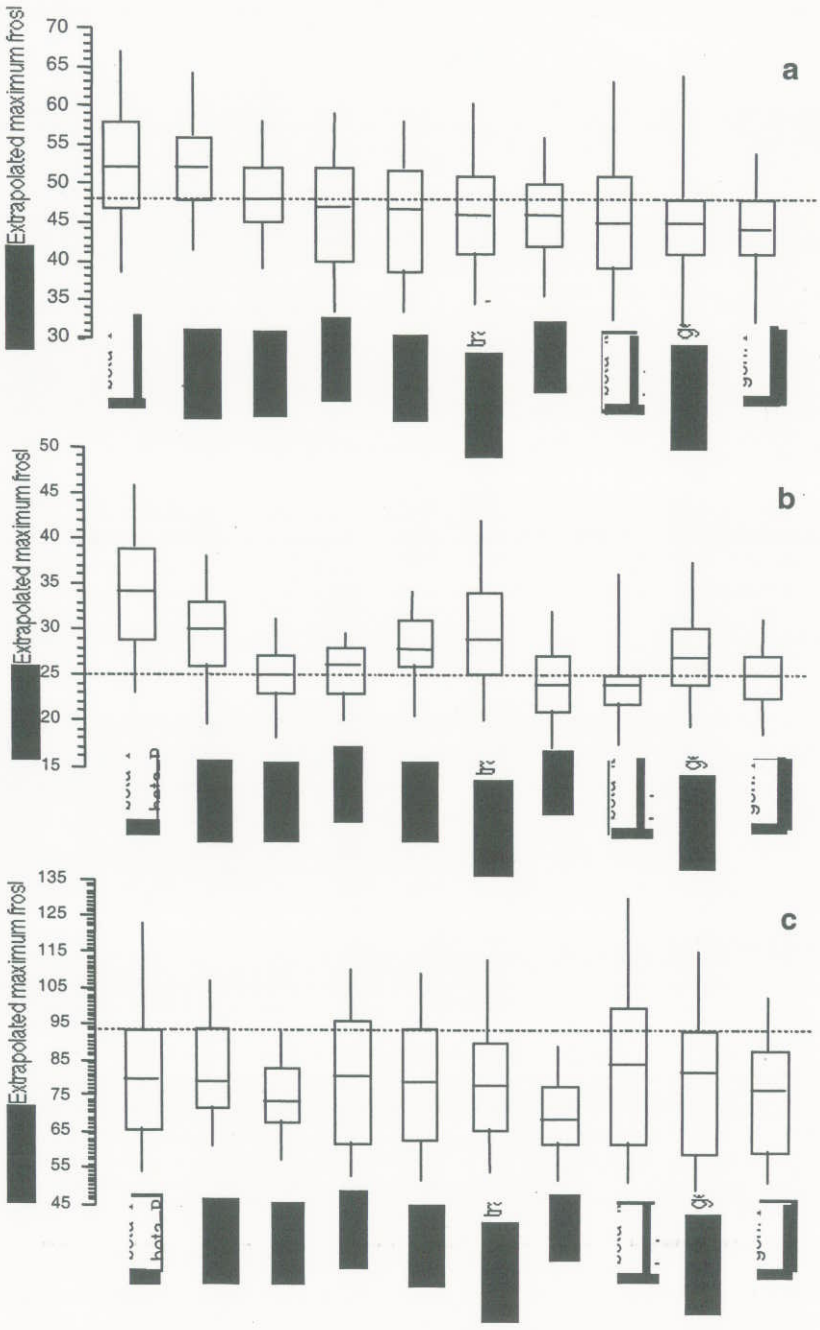

FIGURE 1

Summary of bootstrap results for the deepest modeled annual maximum frost depth at a) Fredonia, NY (N= 67 years, exceedence probability = 0.0147); b) Langley, VA (N= 59 years, exceedence probability = 0.0167); and c) Caribou, ME (N= 57 years, exceedence probability = 0.0172). The actual value at each station is indicated by the dotted horizontal line. Boxplots show the 5th, 25th, 50th, 75th and 95th percentiles of the distributions of extrapolations to the appropriate exceedence probability, from distributions fitting using random samples of size 30.

At Fredonia (Fig 1a), the median for the Gumbel matches the empirically derived extreme value, while the medians for the other distributions either overestimate (beta-P and Revfeim) or more commonly underestimate the empirical value. Sampling variations are also minimized by the Gumbel at this site as evidenced by the relatively compact boxplot for this candidate distribution. Similar results are obtained for Langley (Fig. 1b). In this case, the medians of both the Gumbel and generalized gamma match the observed extreme. The medians of the other candidate distributions generally overestimate the empirical extreme. Sampling variability is also minimized by both the Gumbel and generalized gamma making both attractive candidate distributions. However, the smaller interquartile range exhibited by the Gumbel, makes this distribution more desirable. Although the beta-κ exhibits an even smaller interquartile range, its slight bias toward underestimation of the target maximum frost depth and its relatively large overall sampling variations make this distribution less desirable.

Each of the candidate distributions underestimates the observed frost depth extreme at Caribou, by 10% in the case of beta-κ to 26% for the GEV distribution (Fig. 1c). Although the underestimation of the target frost depth is minimized by beta-κ, its bootstrap distribution exhibits the largest sampling dispersion. A similar pattern of relatively small negative bias, but large sampling variability is present in several of the other bootstrap distributions. Although the Gumbel underestimates the empirical extreme by 20%, this distribution exhibits the smallest sampling dispersion. As a result, with the exception of the Revfiem, this distribution also minimizes the negative bias associated with the lower quartile and 5th percentile of the bootstrap distribution. Given that each distribution exhibits a negative bias, these features make the Gumbel one of the more desirable distributions for extrapolating extreme frost depths at Caribou.

A possible reason for the inferior performance of all the distributions at Caribou may stem from the relatively short period of record (57 years). It is possible that the observed frost depth extreme during this period is associated with a return interval much in excess of the available period of record. In this case, any extreme value distribution (with the possible exception of those which would grossly overestimate the target frost depth) would exhibit substantial negative bias when evaluated using the bootstrap procedure. This supposition is supported somewhat by the annual maximum frost depth observations at Caribou. While two deepest frost depths observed at Caribou exceed 90 cm, the third most extreme soil freezing depth does not exceed 60 cm. Given this discontinuity between the second and third largest frost depths, the bootstrap procedure was repeated using the third largest modeled annual maximum frost depth and an exceedence probability corresponding to two years less than the sample size (0.0179). These results are shown in Figure 2.

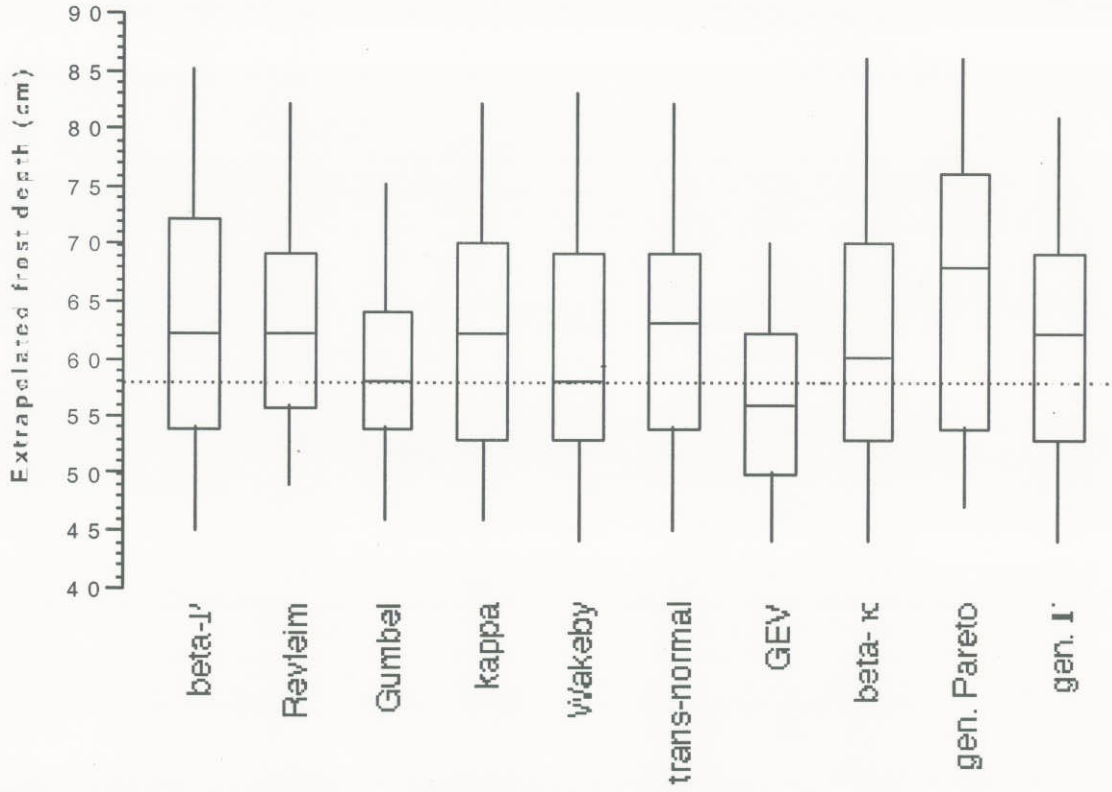

FIGURE 2
As in Figure 1, but for the third deepest annual maximum frost depth at Caribou, ME (exceedence probability = 0.0.182).

When the third deepest maximum frost depth at Caribou is considered, the median for the Gumbel matches the empirically derived extreme value, while the medians for the other distributions either overestimate or, in the case of the GEV, underestimate the empirical value. Sampling variations are also minimized by the Gumbel making this the most desirable distribution. Based on this analysis for Caribou, the results for the 3 sites in Figure 1, and the advantage of selecting a single regionally representative distribution, the Gumbel distribution was chosen as the best candidate distribution for representing annual maximum soil freezing extremes.

MAXIMUM FROST DEPTH CLIMATOLOGY

Data

Annual model-derived maximum frost depths were calculated for a set of 3000 U.S. cooperative network stations. To be included in the 2-, 5-, 10-, or 25-year climatologies, stations were required to have at least 10 years of non-missing daily climatological data. Data requirements of 19 and 29 years were imposed for the 50- and 100-year climatologies, respectively. At all sites serially complete daily temperature data (DeGaetano et al., 1995) were available for the 1951-1997 period. Serially complete snow depth and precipitation data were not available. If missing, these parameters were estimated in a manner similar to that used with the stations selected for screening the candidate extreme-value distributions. As in the bootstrap screening procedure,

years were not considered if any missing data values occurred for more than 14 consecutive days during October through April. In all cases, the meteorological data were required to pass the quality-control procedure of Robinson (1993)

Computation of Return Periods

Smoothing and extrapolation of the modelled annual maximum frost depth data for all stations was accomplished by fitting the Gumbel distribution (Wilks, 1995). The probability density function for this distribution is

$$f(x) = \frac{1}{\beta}\exp\left\{-\exp\left[-\frac{(x-\xi)}{\beta}\right]-\frac{(x-\xi)}{\beta}\right\}, \quad (1)$$

where x is the random variable (in this case, annual maximum frost depths), which must be nonnegative. The distribution has two parameters: ξ is a location parameter, and β is a scale parameter. Separate distributions are fit to the data for each station by maximum likelihood, using the Levenberg-Marquardt method (Press et al., 1986). One convenient feature of the Gumbel distribution is that it is analytically integrable, so that its cumulative distribution function can be written in closed form. That is, Gumbel probabilities can be obtained using

$$F(x) = \Pr\{X \le x\} = \int_0^x f(x)dx = \exp\left\{-\exp\left[-\frac{(x-\xi)}{\beta}\right]\right\}. \quad (2)$$

Average return periods, R, relate to cumulative probabilities, F, of the distributions of annual maximum data according to

$$R = \frac{1}{\omega[1-F(x)]}, \quad (3)$$

where ω is the average sampling frequency, in this case 1 yr^{-1}. Subsequently, frost depths, x, corresponding to specified return intervals are obtained by solving Equation 2 for x and substituting the expression $F(x) = 1 - 1/R$, obtained by rearrangement of Equation 3. These operations yield the expression for frost depths as a function of return period and the parameters of the fitted Gumbel distribution,

$$x = \xi - \beta\ln[-\ln(1-\frac{1}{R})]. \quad (4)$$

Return Period Mapping

Maps depicting the spatial distributions of maximum frost depths for specific return intervals were prepared by first gridding the individual station values, and then producing contour maps from the gridded fields by automated means. A Cressman objective analysis was used to cast the station-specific frost depths to a grid. In the analysis, multiple passes were made through the grid

at sequentially lower radii of influence. For each pass, new values are computed for each grid point based on the station-specific values contained within the radius being considered. Errors (observed station – interpolated station) are determined at each station and used to adjust t he grid point values within the radius being considered.

Appendix B shows maps of the 2-, 5-, 10-, 25-, 50-, and 100-year return periods for maximum annual frost depth under bare soil and sod using observed snow cover conditions. Separate maps are also shown for snow-free bare soil conditions.

SENSITIVITY TO SOIL CHARACTERISTICS

The frost depths shown in Appendix B depict results for soils having a clay content of 10%, a field capacity of 30% and a porosity of 45%. Non-clay soil particles are assumed to be quartz-based. In order to quantify the effect of differing clay contents and porosities on annual maximum frost depths, a geographically representative set of 401 stations was selected. These sites represent those with at least 40 years of non-missing data. At each of these sites separate frost depths corresponding to the 2-, 5-, 10-, 25-, 50- and 100-year return intervals were calculated using soil porosities ranging from 25 to 55% in increments of 10% and field capacities in the range of 15 to 45%. Similarly frost depths were computed for clay contents of ranging from 5 to 30%, holding porosity constant at 45% and field capacity at 30%.

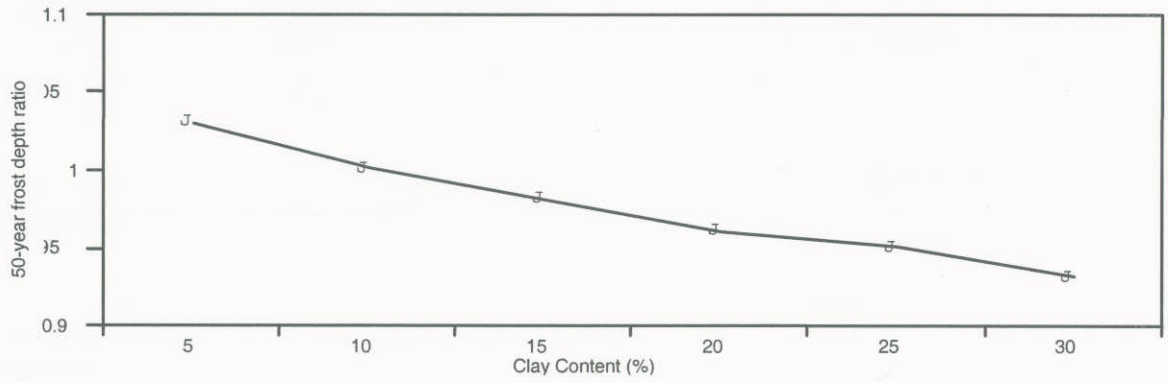

FIGURE 3
Graph of adjustment factors (percent of the maximum frost depth using a standard soil porosity of 0.45 and 30% field capacity) used to convert the maximum frost depth values presented in Appendix B to values representative of a site-specific soil clay content.

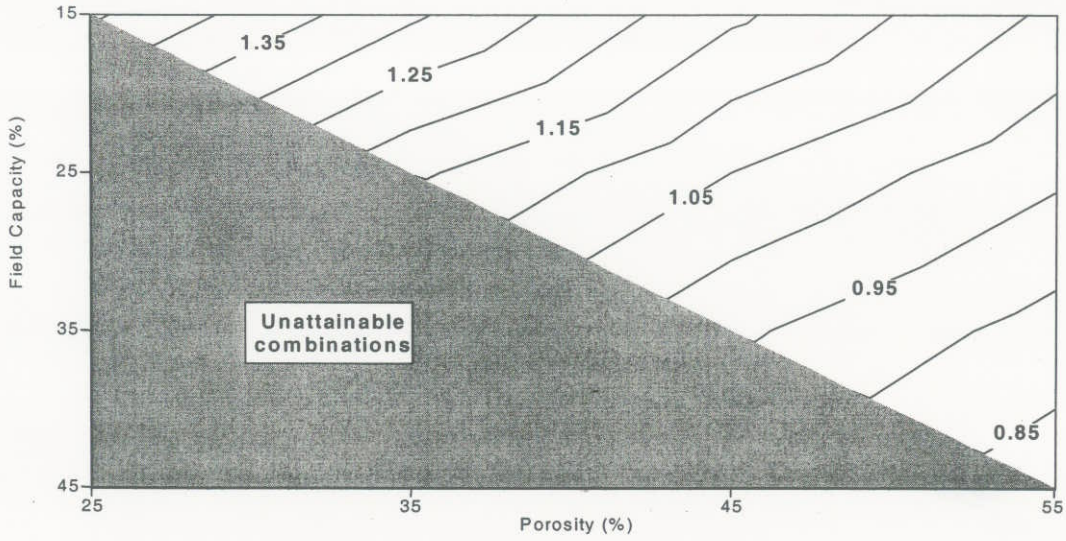

FIGURE 4
Contour graph of adjustment factors (percent of the maximum frost depth using a standard soil porosity of 0.45 and 30% field capacity) used to convert the maximum frost depth values presented in Appendix B to values representative of a site-specific porosity and field capacity values.

Modification of the clay content had little effect on the depth of soil freezing. In general, the difference in maximum soil freezing depth between the standard (10% clay content) and either clay content extremes (5 or 30%) was less than 7% (Fig. 3). Changes in porosity and field capacity, and thus water content, had a more pronounced effect on the maximum depth of frost penetration. Figure 4 shows these differences in the 50-year return period frost penetration as a ratio of the annual maximum freezing depth based on the given porosity to that which occurred using the standard 45% porosity, 30% field capacity combination. Figure 5 shows the station-to-station differences in these ratios was quite small (generally _ 0.10) as were the return-period-to-return period differences..

With two exceptions, the ratios shown in Figure 4 are generally within 12% of 1.0. In the driest and most compact case (15% field capacity and 25% porosity) the 50-year return period frost depth is over 40% deeper than that of the base case. Increasing the porosity to 35% and the field capacity to 25%, yields a 16% increase in the 50-year return period frost depth. Frost depths tend to decrease at field capacities and porosities greater than the base case. In application, Figure 4 can be used to adjust the maximum frost depth values presented in Appendix B to values representative of a site-specific soil porosity and field capacity.

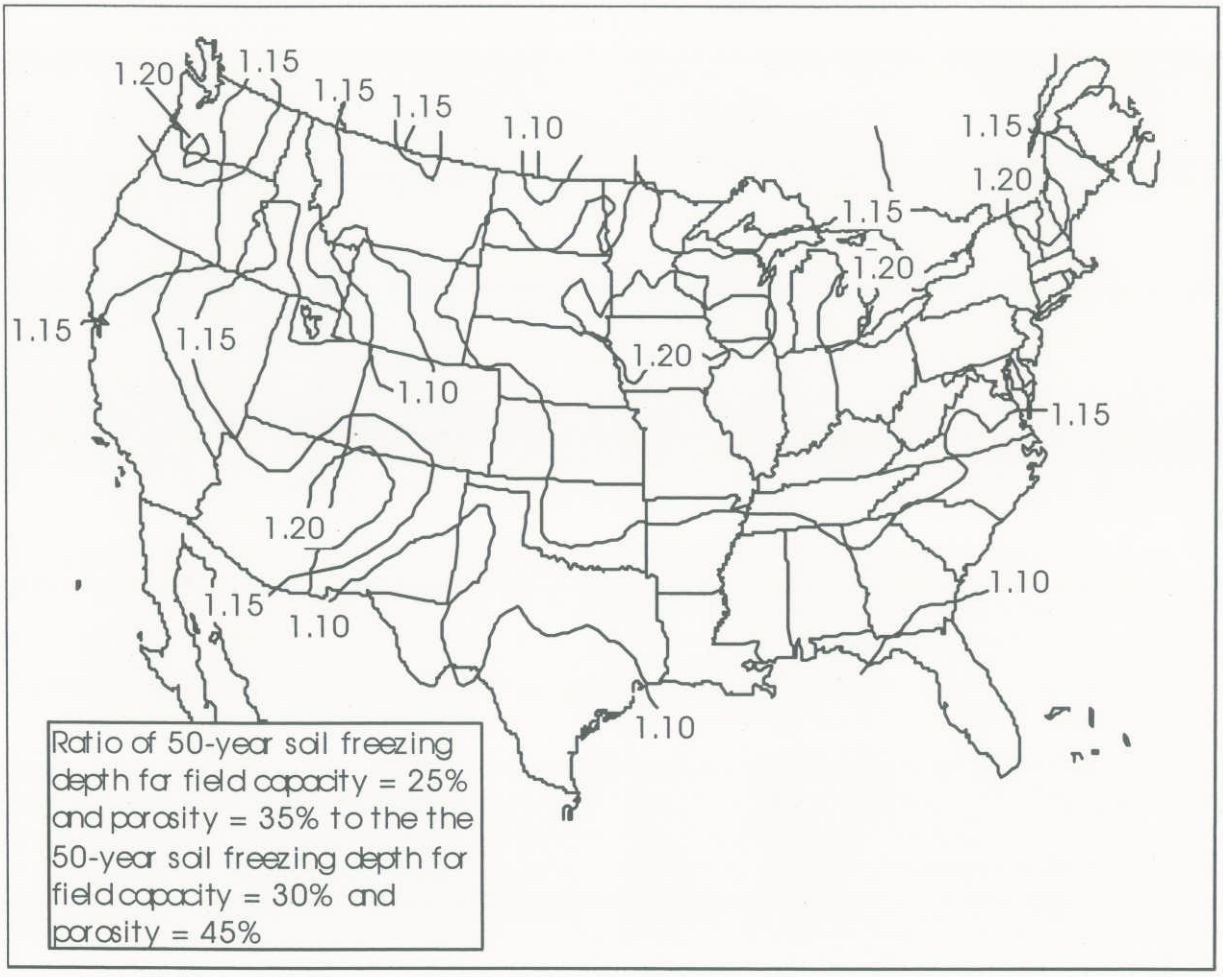

FIGURE 5
Spatial distribution of adjustment ratios used to compile Figure 4.

REFERENCES

Crandell, J.H., Lund, E.M., Bruen, M.G., and Nowak, M.S. (1994). "Design guide for frost-protected shallow foundations." Report available from the National Homebuilders Association Research Center, 400 Prince George's Blvd., Upper Marlboro, MD 20772.

DeGaetano, A.T., Eggleston, K.L., and Knapp, W.W. (1995). "A method to estimate missing daily maximum and minimum temperature observations." *J. Appl. Meteor.*, 34, 371-380.

DeGaetano, A.T., Wilks, D.S., and McKay, M. (1996). "A physically-based model of soil freezing in humid climates using air temperature and snow cover data." *J. Appl. Meteor.*, 35, 1009-1027.

Hosking, J.R.M. (1991). "FORTRAN Routines for Use with the Method of L-Moments." Research Report RC-17097, IBM Corp, Yorktown Heights, NY, 117 pp.

Hosking, J.R.M., and Wallace, J.R., (1993). "Some statistics useful in regional frequency analysis." *Water Resour. Res,* 29, 271-281.

Houghton, J.C., (1978). "Birth of a parent: The Wakeby distribution for modeling flood flows." *Water Resour. Res,* 14, 1105-1109.

Press, W.H., Teukolsky, S.A., Vetterling. W.T., and Flannery, B.P. (1992). "Numerical Recipes in FORTRAN The Art of Scientific Computing 2nd Ed." Cambridge University Press, New York, N.Y., 963 pp.

Robinson, D.A., (1993). "Historical daily climatic data for the United States." Preprints American Meteorological Society Eighth Conference on Applied Climatology, Anaheim, CA, 264-269.

Schmidlin, T.W., Edgell, D.J., and Delaney, M.A. (1992). "Design ground snow loads for Ohio" *J. Appl. Meteor.*, 31, 622-627.

Simiu, E., Filliben, J.J., and Shaver, J.R. (1982). "Short-term records and extreme wind speeds." J. Struct. Div., 108, 2571-2577.

USDA, (1941). " Climate and Man, Yearbook of Agriculture 1941." U.S. Government Printing Office, Washington, DC, 1248 pp.

Wilks, D.S., (1993). "Comparison of three-parameter probability distributions for representing annual extreme and partial duration precipitation series." *Water Resour. Res,* 29, 3543-3549.

Wilks, D.S., (1995). "Statistical Methods in the Atmospheric Sciences." Academic Press, San Diego, CA, 464 pp.

Wilks, D.S. and McKay, M. (1996) "Extreme-value statistics for snowpack water equivalent in the northeastern United States using the cooperative observer network" *J. Appl. Meteor.*, 35, 706-713.

PHYSICAL SIMULATION OF MAXIMUM SEASONAL SOIL FREEZING DEPTH IN THE UNITED STATES USING ROUTINE WEATHER OBSERVATIONS

Arthur T. DeGaetano, Michael D. Cameron, and Daniel S. Wilks

Northeast Regional Climate Center

Cornell University, Ithaca, NY 14853

Submitted to:

Journal of Applied Meteorology

November 1999

Revised March 2000

Corresponding author address:

Dr. Arthur DeGaetano, Northeast Regional Climate Center

Cornell University, 1115 Bradfield Hall, Ithaca, NY 14853

email: atd2@cornell.edu

Abstract

An existing physically-based soil freezing model applicable to humid climates is modified for use in the central and western United States. Simulations using the state-of-the-art Simultaneous Heat and Water (SHAW) model indicated that the original model required addition of a water budgeting scheme and alteration of the equation for soil thermal conductivity. Using only daily temperature, liquid precipitation, snowfall and snowcover, this new model allows the simulation of maximum seasonal frost depths at several thousand U.S. stations.

Comparison of the model-derived maximum frost depths with observed and soil temperature-inferred soil freezing maxima at 32 arid and semi-arid locations indicates excellent agreement. Observed maximum soil freezing depths, ranging from 0 to over 100 cm, are simulated with an average absolute error of 5.4 cm. At individual stations, the seasonal penetration and thawing of soil freezing tracks that of the observations quite closely, regardless of ambient soil moisture conditions.

1. Introduction

Information regarding the presence and maximum penetration of soil freezing is necessary for a variety of climate-sensitive engineering applications. The depth of soil freezing varies greatly from season to season and region to region. As a result, building codes must consider the extreme freezing penetration events to assure that footings and utilities are buried at an adequate depth. In addition, information on soil frost penetration is relevant in agricultural (e.g. van Es et al. 1998) and flood forecasting (Molnau and Bissell 1983) applications. Given this relevance, it is not surprising that many methods have been developed for estimating soil freezing. The methods described by Berggren (1943), Harlan (1973), Cary et al. (1978), Benoit and Mostaghimi (1985), Gusev (1985), Flerchinger and Saxton (1989) Jansson (1991) and Gusev and Nasonova (1997) provide an idea of the history and range in complexity of soil freezing models. Kennedy and Sharratt (1998) compared the performance of four of these soil freezing models and found that the finite difference models of Flerchinger and Saxton (1989) and Jansson (1991) simulated maximum frost depth with reasonable accuracy, while the heat flux balance methods of Benoit and Mostaghimi (1985), Gusev (1985) tended to overpredict frost depth.

Despite the relevance of frost depth information and the lack of in-situ frost depth observations, few have attempted to create a model capable of simulating maximum frost penetration at a nationwide network of stations. National scale soil freezing maps appear in the 1941 *Yearbook of Agriculture* (USDA 1941) and Sowers (1979). Unfortunately, the data used in these maps are unofficial, unreferenced and/or antiquated (1899-1938). A related national climatology of 100-year return period air freezing indices was developed by Steurer and Crandell (1995). Using this value, maximum annual soil freezing depths can be inferred based on the Berggren Equation (Berggren 1943).

Although empirical and relatively simplistic, the Berggren Equation is perhaps the best candidate for developing a model-derived national seasonal maximum frost climatology, given its

reliance on only air temperature. The model is an empirically-based expression relating the maximum depth of frost penetration in a given winter, x (m) to the air freezing index , I, (°C degree-days) by:

$$x = \lambda\left(\frac{1.728\times10^{5}\,KnI}{L}\right)^{0.5}, \qquad (1)$$

where λ is a dimensionless coefficient representing soil and ground cover-dependent thermal parameters, K is average thermal conductivity (W m^{-1} $°C^{-1}$), n equals a dimensionless factor to convert I from air to ground surface conditions, and L is the volumetric latent heat of fusion (Jm^{-3}).

For many applications, the Berggren Equation estimates the winter maximum frost depth with sufficient accuracy (Gel'fan 1989). However, the model requires that snow depth be assumed constant and neglects seasonal changes in soil water content. These assumptions are unrealistic in many parts of the United States. Furthermore, model output is limited to the maximum depth of soil freezing, precluding its use in applications where the daily progression of frost depth is required.

These limitations are addressed by physically-based soil freezing models such as the Simultaneous Heat and Water (SHAW) model (Flerchinger and Saxton 1989; Flerchinger 1991; Flerchinger et al. 1994; Flerchinger et al. 1996). The state-of-the-art SHAW model was designed for hydrological applications and thus considers such factors as evaporation, snow depth, runoff and soil water profiles in addition to soil-freezing depth. The model assumes a one-dimensional vertical soil profile, which extends upward through multiple layers representing undisturbed soil, tilled soil (a maximum of 20 soil layers can be considered), vegetative residue, snow, and the plant canopy. Required meteorological and site characteristic input to the model are extensive (Table 1). Based on hourly (or daily) meteorological observations, heat and moisture fluxes can be obtained for the upper model boundary, which in turn are used to compute the fluxes between layers.

Equations in the model are solved implicitly with the Newton-Raphson method (Flerchinger and Saxton 1989).

As opposed to the empirical Berggren approach, the amount of water in the soil is an integral part of the SHAW model's simulation of the daily progression of soil freezing. In addition to the effect of soil moisture on soil thermal conductivity and latent heat release during freezing, water movement also plays a role in the process of soil freezing, particularly when the soil is near saturation. Water has a tendency to be attracted to the boundary between frozen and unfrozen soil. Movement of water to this freezing front results from thermal gradients which induce water potential gradients within the soil and thus further water movements.

Although the SHAW model addresses each of the relevant physical processes that govern soil freezing, its extensive data requirements limit its use to a very few heavily instrumented locations. An intermediate class of models is referred to as heat flux balance methods by Kennedy and Sharratt (1998). Examples of this type of approach are given by Benoit and Mostaghimi (1985) and Gusev (1985). The data requirements of these approaches can be fulfilled by the data available from the Cooperative Observer network, making them attractive for estimating soil freezing on a national scale. However, in a comparison of the ability of these models to estimate maximum frost depth, Kennedy and Sharratt (1998) found that they tended to overpredict the depth of soil freezing due to their neglect of volumetric heat content. Furthermore, the Gusev (1985) model does not allow for thawing at the soil surface. Although presumably this has only minor consequences for maximum frost penetration, it limits the model's use in other applications.

Based on the frequency of requests for soil freezing information received by the Northeast Regional Climate Center, DeGaetano et al. (1996) developed a physically-based soil freezing model with application to the northeastern United States, (hereafter the NRCC model). The design of the model was guided by the availability of meteorological data at the national network of stations with the greatest spatial density. Thus, meteorological input was limited to

daily maximum and minimum temperature and snow depth. In addition, daily observations of liquid-equivalent precipitation and snowfall were used to empirically estimate snow density from snow depth. The NRCC model can best be classified as an hybrid of the more complex finite-differencing approaches (e.g., SHAW) and the simpler heat flux balance methods. As such, it blends the desirable characteristics of each model group. Meteorological input requirements are limited. However, instead of solving a set of equations representing discrete modes of heat transfer as is done by Benoit and Mostaghimi (1985), the NRCC model employs a coarse finite-differencing scheme, using soil layers of variable depths.

Like both classes of models, the NRCC model assumes one-dimensional heat flow. This is shown schematically in Figure 1. In this figure, depths (m) below or above (in the case of snow and/or air) the surface are indicated by Z and temperatures (°C) are indicated by T. Subscripts indicate snow (s), frozen soil (f), the soil surface (0), and the lower boundary (D). The subscript "y" refers to the value observed or estimated for the previous day. The model assumes that the flux of heat through the lower boundary is negligible. At the lower boundary, Z_D, which is set at a depth of 2 m, a daily "deep" temperature T_D is specified as a function of the average air temperature over a period from the previous April through March following the winter in question, the 25th percentile January through March snow depth for the current winter and the combined thermal diffusivity of the snow and soil. Specifying T_D over the period from April through March assured proper initialization of this boundary temperature prior to the start of the freezing season, while also accounting for the effects of the previous winter on the rate of summer warming. Since weather data for the entire season are used to specify the lower boundary conditions, the model is diagnostic rather than prognostic.

The upper boundary condition is given by the observed average daily air temperature. Here the assumption is made that the average daily air temperature is representative of the temperature of the snow surface. The snow depth (Z_s) gives the thickness of the first layer in the snow/soil system (Fig. 1). In the absence of snowcover, the air temperature is assumed to equal the temperature at the upper surface of a 1.0×10^{-3} m laminar layer, the thermal properties of which are characteristic of

still air. Thus the temperature at the soil surface is prescribed by the model, avoiding the need to incorporate an empirical n-factor as in Equation (1). Progressing downward, soil layers of variable depth are defined by frozen and unfrozen zones, the boundaries of which are at 0°C. A maximum of three soil layers (one frozen and two unfrozen) is allowed by the model.

Temperature gradients through each layer are assumed to be linear, and thus the heat fluxes (Wm^{-2}) at the middles of each layer, Q_x, are defined by the differences between the temperatures of the layer boundaries. Imbalances between the resulting vertical heat fluxes (i.e., heat flux convergence or divergence) are rectified through internal temperature changes and, when these changes cross 0° C, freezing or thawing of an appropriate depth of soil. In this process, the fluxes are balanced by accounting for the heat capacities of soil solids and soil water, and for the latent heat of fusion. This is sketched in Figure 1 and given mathematically for the case when a frozen layer exists at the surface by the governing equations:

$$Q_{snow} = Q_{froz} = Q_{deep}, \tag{2}$$

where

$$Q_{snow} = -K_{snow}(T_s - T_0)/Z_s + \Delta Q_U, \tag{3}$$

$$Q_{froz} = K_{froz}(T_0/Z_f) + \Delta Q_L, \tag{4}$$

and

$$Q_{deep} = K_{thaw}T_D/(Z_f - Z_D) + (Z_{fy} - Z_f)(\phi - 0.1)L_f \tag{5}$$

The variables used in Equation 2-5 have been defined previously, with the exception of the latent heat of freezing (Jm^{-3}), L_f; soil porosity (ϕ); thermal conductivities($Wm^{-1}°C^{-1}$) of snow, K_{snow}, frozen soil, K_{froz}, and unfrozen soil, K_{deep}, and the change in heat storage terms (Wm^{-2}), ΔQ. Equations 2-5 are solved numerically for the prognostic variables T_0 and Z_f. Nearly saturated soil moisture conditions are assumed at all times. This assumption is quite reasonable

during the soil freezing season in the northeastern U.S. In Figure 1, ΔQ_U is represented by the hatched and cross-hatched areas between the two consecutive daily average temperature profiles. Similarly, ΔQ_L is shown by the speckled and dotted regions.

Only one of three possible soil-freezing states is illustrated in Figure 1. In this state, a layer of frozen soil extends from the surface to some depth Z_f. The other possible states are that the soil may remain unfrozen from the surface to the lower boundary, Z_D, or a layer of frozen soil may exist between two layers of unfrozen soil. In addition, five transition modes are possible, corresponding to the transitions between the three basic states with the exception of the transition from unfrozen to a buried frozen layer, which is not physically realizable.

The model is initiated in the unfrozen state and continues in this manner until T_0 falls below 0° C. At this point, the transition to frozen soil mode is activated. Provided the temperature remains below 0° C on subsequent days, the model operates in the frozen soil mode. In this state, both soil freezing and thawing occur at the bottom of the frozen layer. When T_0 exceeds 0° C, the model transitions to either the unfrozen or surface thaw state. In the surface thaw state, the layer of frozen soil is allowed to thaw both from its top and bottom. The temperature throughout the buried frozen layer that results is assumed to be constant at 0° C. For subsequent occurrences of $T_0 < 0°$ C freezing occurs at the both the top and bottom of the buried frozen layer.

Despite favorable correspondence between measured and observed frost depths in the Northeast (DeGaetano, et al. 1996; DeGaetano et al. 1997), the original NRCC model is not applicable across the United States. In particular, winter soil moisture conditions in the more arid north-central and northwestern U.S. can be substantially drier than is assumed by the model. This influences the dynamics of soil freezing very substantially. For example, Figure 2 shows maximum soil freezing depths for the winters of 1984-85 through 1996-97 at Ithaca, New York, as simulated by the SHAW model for different fixed moisture contents. The maximum depth of freezing in each year increases as the water content decreases from 15% (dry) to 5% (extremely dry). A general increase in maximum annual frost depth is noted as water content decreases from 35%

(near saturation) to 15%.

2. NRCC model refinements

For the NRCC model to be applicable in drier climates, it is necessary both to specify the degree of dryness in a given winter, consistent with data limitations, and to capture the effects of lower soil water content on thermal conductivity and reduced latent heating.

a. Water Budget

The methods of Palmer (1965) and Thornthwaite (1948) (also see Alley 1984) were used to compute volumetric soil water content on the spatial scale of climate divisions (Guttman and Quayle 1996). Each state is divided into divisions ranging in number from 1 to at most 10 climate divisions. Divisions generally represent drainage basins or crop-reporting districts. For each division, an average soil profile is defined by two layers. The top layer (SS) contains up to 2.5 cm of soil water, with the remaining soil water contained in the lower (SU) layer. Water first enters the top layer, which must fill to capacity before any water infiltrates into SU. Water leaving the system evaporationally is withdrawn from the top layer first, before being drawn up from below. Precipitation, evapotranspiration, and to some extent runoff, dominate this simple water budget.

Monthly climate division precipitation totals are the source of water input to the budget. These totals represent the average precipitation received at all reporting sites within a division. Climate division precipitation totals are updated operationally on a monthly basis and have been archived from 1895 onward.

Monthly climate division evapotranspiration totals were obtained using the method of Thornthwaite (1948). This empirical procedure assumes a direct relationship between monthly average temperature, $\overline{T}$, and incoming solar radiation. Evapotranspiration is assumed to be negligible at $\overline{T} < 0°C$ and is set at the maximum potential rate when $\overline{T} > 26.5°C$ (Sellers 1965). At

intermediate temperatures, monthly potential evapotranspiration (cm), ET_P, is simply a function of $\overline{T}$ (°C). Rosenberg (1974) gives a thorough explanation of the calculation of ET_P using the Thornthwaite approach.

The value of ET_P given by Thornthwaite's method is based on 12 hours of daylight and maximum soil moisture availability. Therefore corrections for day length and soil moisture deficit are applied to obtain the actual monthly evapotranspiration total ET. The daylength correction is the average monthly hours of daylight divided by 12, while the soil moisture correction is the ratio of actual to saturated volumetric water content (Palmer and Havens 1958). Based on these values of ET and precipitation, changes in monthly soil water content are tracked using a bookkeeping approach. Soil moisture recharge occurs when precipitation (P) exceeds ET, with the new soil moisture expressed as the sum of the previous month's moisture content and the difference (P - ET). When recharge exceeds the soil's capacity for holding water, the excess water is lost as runoff.

In months having ET > P, water loss from SS is given by

$$L_{SS} = \min[S_{SS-1}, (ET-P)], \tag{6}$$

where S_{SS-1} is the amount of water present in the surface layer during the previous month. Losses from the underlying layer follow from

$$L_{SU} = [(ET-P) - L_{SS}]\, S_{SU-1}/AWC \tag{7}$$

where, S_{SU-1} is the amount of water present in the underlying layer during the previous month, and the available water holding capacity (AWC) is the maximum water storage for the soil. A value for AWC is assigned to each climate division as part of Palmer's procedure.

In all cases, precipitation falling during months with $\overline{T} < 0$°C, is assumed to be frozen and thus is not available for soil moisture recharge. This moisture is held in storage through the winter and

becomes available during the first month, *j*, satisfying the condition:

$$0.5(T_j + T_{j-1}) > 0°C. \quad (8)$$

Since water is assumed to be evenly distributed through each of the soil horizons, the volumetric water content, θ (m^3m^{-3}), can be expressed by

$$\theta = \phi\,[(S_{SS} + S_{SU})/AWC],\ 0 < \theta \leq FC \quad (9)$$

where S_{SS} and S_{SU} are the water storage in the surface and underlying layers after following the bookkeeping approach during the current month and ϕ is soil porosity. In near-saturated conditions the soil usually drains quickly to field capacity *FC*. This value, which can be obtained from USDA soil surveys, is used as an upper limit for θ.

Use of the Palmer soil water budget requires information concerning the previous month's soil moisture storage. This is problematic when initializing the budget. To address this issue, an iterative scheme was developed to search through the precipitation and evapotranspiration data for the earliest month when precipitation exceeded the sum of available water capacity and monthly evapotranspiration. The budget could then be initialized at AWC during this month. When a single month meeting this criterion could not be identified, the search and initialization procedure were applied using two- or three-month precipitation and evapotranspiration totals. In all climate divisions, the water budgets were initialized prior to 1930.

ii. Thermal conductivity adjustment

The original NRCC model uses the approach of Farouki (1986) to compute soil thermal conductivity. This approach works well for moist soils, but breaks down for dry conditions. Here, thermal conductivity is computed as a function of soil moisture,θ, using Campbell's (1985) equation

$$K_{deep} = A + B\theta - (A - D)\exp\left[-(C\theta)^{E}\right] \tag{10}$$

where K_{deep} is the thermal conductivity of the unfrozen soil system and A, B, C, D, and E are empirical constants related to soil type (Campbell 1985).

The constant A is expressed as a function of the volume fractions of quartz, φ_q, clay, φ_m and all solids φ_s as:

$$A = \frac{0.57 + 1.73\varphi_q + 0.93\varphi_m}{1 - 0.74\varphi_q - 0.49\varphi_m} - 2.8\varphi_s(1 - \varphi_s). \tag{11}$$

The empirical expression for the term B is:

$$B = 2.8\varphi_s\theta, \tag{12}$$

while the term C is defined:

$$C = 1 + 2.6m_c^{-0.5} \tag{13}$$

where m_c is the mass fraction of soil comprised of clay. Physically, term C determines the critical water content at which thermal conductivities begin to increase rapidly with increasing volumetric water content (Campbell 1985). The mass fraction of clay can be found from the volume fractions of both the quartz and clay and their bulk densities with the weighting expression:

$$m_c = \frac{2.65\varphi_m}{(2.65\varphi_m + 2.66\varphi_q)} \tag{14}$$

The D term is:

$$D = 0.03 + 0.7\varphi s^2 \tag{15}$$

The E term is typically around 4.0, as validated through experimentation, and Δz is the depth of the soil layer (2.0 m) (Campbell 1985).

In the case of frozen soil, the thermal conductivity, K_{froz}, is adjusted using:

$$K_{froz} = 3.82\theta K_{deep}, \tag{16}$$

where 3.82 is the ratio of the thermal conductivities of ice (2.18 W $m^{-1}°C^{-1}$) and pure water (0.57 W $m^{-1}°C^{-1}$).

Since water content can vary through the winter, thermal conductivity is recalculated during each month. The median thermal conductivity (April - March) is used to calculate the deep temperature wave.

3. Refined model validation

Frost depth measurements at several central and western U.S. sites were available for comparison with the revised NRCC model simulations. Temperature and precipitation (both liquid and snow) data for these sites were available from co-located National Weather Service Cooperative Observer Network stations. Soil characteristics were determined using USDA soil survey data.

a. Reynolds Creek Watershed, Idaho

Extensive soil freezing studies conducted in the 1970s and 1980s at several observation sites in the Reynolds Creek Watershed of southwestern Idaho provided the most thorough set of available verification data. Data from three sites, Reynolds Creek, Reynolds Mountain and Lower Sheep Creek were used. Since a cooperative station is co-located with the Reynolds Creek observation

site, daily snowpack and snowfall data were available there. Daily snowpack and snow fall data were not available for Reynolds Mountain or Lower Sheep Creek, but were estimated from the approximately bi-weekly snow observations reported by Hanson et al. (1988). At each site soil characteristics were described by $\phi = 0.40$, FC=0.30 and φ_m=0.2.

Simulations based on the Reynolds Creek weather data verified the revised NRCC model's ability to model maximum frost depths, timing of maximum depths and progression of frost depths through the course of winter. Representative trials for the 1977-1978 and 1978-1979 winter seasons are shown in Figures 3 and 4. Minimal soil freezing was observed during the winter of 1977-1978 (Fig. 3). During this winter maximum modeled and observed soil freezing occurred in late November, with the observed maximum depth reaching 14 cm and the modeled depth at about 17 cm. Through most of December, both the model and observations indicate frost-free conditions. A short period of frozen soil is simulated by the model in early January (14 cm depth) and confirmed by the observations (9 cm depth). The week-long period of shallow (< 10 cm) frozen soil given by the model in late December is not evident from the observations. During each of these three periods, the frost depths simulated by the original NRCC model are similar to the revised values, despite rather dry (10% water content in December) soil moisture conditions.

Figure 4 shows a winter experiencing prolonged and relatively deep soil freezing. During this winter the simulation shows remarkable correspondence to the observed frost depths. In both cases, soil freezing was initiated in early November, with frozen conditions remaining almost uninterrupted through late February. With regard to the maximum frost depth, the model-derived depth of 74 cm compares favorably with the 80 cm observation. Both the observed and modeled value occur on February 4. The original NRCC model gives a much deeper (104 cm) frost depth during this dry ($\theta = 0.10$) winter.

The sensitivity of several of the parameterizations incorporated into the revised model

were evaluated using data from the two seasons presented in Figures 3 and 4. Table 2 shows the results of this analysis for the five empirical coefficients used in the Campbell (1985) conductivity equation as well as θ, φ_m and ϕ. In each trial, these eight parameters were increased (or decreased) from their original value by 20 and 50%. Overall, the model is most sensitive to ϕ, as a 20% change in this value results in as much as an 18% difference in maximum frost depth. Although a 20% change in the coefficient C, produces a 11% change in maximum frost depth during 1977-78 (Fig. 3), changing this parameter had little effect the model output during 1978-79, when the freezing was extensive. A similar disparity was found for φ_m. This is expected given the reliance of C on clay content. A 20% modification of the A coefficient or θ, resulted in a change of maximum soil freezing deep of about 5%, while a larger 50% perturbation of these parameters was associated with frost depth differences in the range of 6 to 10%.

Collectively, it appears that the model is most sensitive to the proportion of soil volume comprised of air and water. Misspecification of φ_m and Campbell's A coefficient account for relatively small (about 10%) differences in the estimated frost depth. This is in agreement with a more extensive analysis of the sensitivity of the original NRCC model to differences in φ_m and ϕ given by DeGaetano et al. (1997), which found at most a 5% change in the maximum depth of soil freezing for clay contents in range of 2 to 50%. Given these results and the lack of site-specific soil information at most weather stations, it would be prudent to compare frost depths based on a range of porosities to characterize the uncertainty due to differences in the assumed ϕ value.

Trials conducted at Reynolds Mountain and Lower Sheep Creek, Idaho also matched the observations relatively well. Unfortunately, the lack of daily snow data required that snow input be extrapolated, which clearly introduces error into the comparisons. Only maximum frost depths were analyzed for this reason. Nonetheless, modeled maximum frost depths consistently occurred within three days of the observed maximum frost depths

for the three freezing seasons simulated. During these seasons, which correspond to the data given by Hanson et al. (1988), the differences between observed and modeled maximum frost depth averaged 5.0 cm and 6.7 cm at Lower Sheep Creek and Reynolds Mountain, respectively (Fig. 5). The consistent overestimation of maximum frost depth at Reynolds Mountain, is likely due to spatial variations in snow depth between the frost depth and precipitation observation sites. Clearly, the ability to spatially interpolate soil freezing depth estimates in mountainous regions is complicated by these microclimatic differences.

b SCAN Sites

Soil Climate Analysis Network (SCAN) sites at or near cooperative weather stations provided a source of verification data based on observed soil temperatures at 5, 10, 20, 50 and 100 cm depths. From these hourly or (6-hourly) data, the depths of the 1, 0, and -1^{O}C isotherms were linearly interpolated. This ±1^{O}C isotherm band about the freezing point delineated reasonable bounds on the position of the 0^{O}C isotherm.

i. Lind, Washington.

Modeled and soil-temperature-inferred frost depths at Lind, Washington show close agreement throughout the 1994-1955 winter (Fig. 6) This winter was characterized by several distinct penetrations of the 0°C isotherm which were captured by the revised NRCC model. Based on the model, the maximum frost depth of 25.4 cm occurred in early January. Despite capturing the timing of maximum soil freezing reasonably well, this is somewhat shallower than the 35 cm maximum depth of the interpolated 0°C isotherm. Nonetheless the modeled maximum frost depth remains within the ±1°C envelope about the freezing isotherm.

ii. Mandan, North Dakota

Verification results using Mandan, North Dakota data for 1996-1997 provided another example of the revised NRCC model's ability to accurately simulate frost penetration and maximum soil freezing in semi-arid climates (Fig 7). During this snowy winter, the modeled soil freezing level remains relatively constant at about 25 cm from late November through the end of March. The interpolated $0^{o}C$ isotherm shows a similar pattern, particularly during the latter three months. Although similar in magnitude, the modeled maximum frost depth level of 32.2 cm occurs much earlier in the season than 37 cm maximum depth of the inferred 0°C isotherm.

c. Midwest frost gauge observations

Frost gauge data (Ricard et al. 1976) collected at DeKalb, Illinois during the 1998-1999 winter provide a final verification of the revised NRCC model. During this winter, with nearly saturated soil moisture conditions, the modeled frost depths once again track the observations quite closely (Fig. 8). The maximum simulated frost depth of 30.4 cm agrees with the measured 23 cm maximum, but occurs about 10 days earlier. However, the timing of the initiation of soil freezing in December and the late January thaw are both captured by the model. The consistent overestimation of soil freezing through the season relates to the rapid onset and penetration of soil freezing. In this case it is likely that the temperature of the soil surface was initialized too cold in the model producing deeper-than-observed soil freezing.

4. Summary

To be applicable on a national scale, the Northeast Regional Climate Center frost depth model was modified through the addition of a soil moisture budget and refinement of the

model's thermal conductivity equation. Based on model performance in near-saturated conditions and SHAW model simulations for dry soil, freeze-induced migration of water to the frozen-unfrozen boundary continued to be ignored in the revised model. This allowed the meteorological data requirements to be limited to daily temperature, precipitation (both snow and liquid equivalent) and snow cover. These data are available nationally at a relatively dense spatial resolution.

The incorporation of a water budget into the model was also predicated by these data limitations. The methods of Palmer (1965) and Thornthwaite (1948) were used to estimate soil moisture content at monthly temporal resolution. These methods use a bookkeeping approach to account for monthly variations in soil water content. Soil recharge is limited to observed precipitation, while evaporation is the sole source of water loss. Monthly evapotranspiration can be inferred using only temperature and station latitude based on the Thornthwaite method.

The ability of the revised NRCC model to simulate seasonal maximum frost depth is exceptional based on comparisons of modeled and observed soil freezing levels at various western and central U.S. sites. The verification results given in Figure 9 clearly support this assertion. Here the results of 32 verification trials at western and central U.S. stations are summarized. The values at all sites fall along the 1:1 line, with mean difference (i.e. bias) of only 1.4 cm and a mean absolute difference of 5.4 cm, based on the observed frost depth sites. Both relatively shallow and deeper frost depths are estimated with similar absolute accuracy, yielding an average percent difference of 11%, but better relative performance for the more significant events. These results indicate that the revised NRCC model can be used to develop a national soil freezing climatology.

5. Acknowledgments

This work was sponsored by the National Association of Homebuilders (NAHB) and the U.S. Department of Housing and Urban Development through a cooperative agreement with the NAHB

Research Center, Inc. Partial support was also provided through NOAA Cooperative Agreement NA67RJ-0146. We are indebted to Gerald Flerchinger for providing us with the SHAW model and extensive help with parameterizing the model for compatibility with the NRCC model runs. Thanks also go to David Changnon and Nolan Doesken for diligently installing frost tubes and collecting soil freezing data at their weather stations.

6. References

Alley, W.M., 1984: The Palmer Drought Severity Index: Limitations and Assumptions. *J. Climate Appl. Meteor.*, **23**, 1100-1109.

Benoit, G. R. and S. Mostaghimi, 1985: Modeling Soil Frost Depth under Three Tillage Systems. *Trans. of the ASAE*, **28**, 1499-1505.

Berggren, W.P., 1943: Prediction of temperature distribution in frozen soils. *Trans. of Amer. Geo. Union*, **3**, 71-77.

Campbell, G.S., 1985: *Soil Physics with BASIC.* Elsevier, 150 pp.

Cary, J.W., G.S. Campbell and R.I. Papendick, 1978: Is the soil frozen or not? an algorithm using weather records. *Water Resour. Res,* **14(6)** 1117-1122.

DeGaetano, A.T., Wilks, D.S. and M. McKay, 1996: A Physically-based model of soil freezing in humid climates using air temperature and snow cover Data. *J. Appl. Meteor.*, **35**, 1009-1027.

DeGaetano, A.T., Wilks, D.S. and M. McKay , 1997: Extreme-Value Statistics for Frost Penetration Depths in Northeastern United States. *J. of Geotech. and Geoenviro. Eng.*, **123**, 828-835.

Farouki, O.T., 1986: *Thermal Properties of Soils.* Trans-Tech Publications, 136 p.

Flerchinger, G.N., 1991: Sensitivity of Soil Freezing Simulated by the SHAW Model. *Trans. of the ASAE*, **34**, 2381-2389.

Flerchinger, G.N. , Baker, J.M., and E.J.A. Spaans, 1996: A Test of the Radiative Energy Balance of the SHAW Model for Snowcover. *Hydr. Process.*, **10**, 1359-1367.

Flerchinger, G.N, Cooley, K.R., and Y. Deng, 1994: Impacts of spatially and temporally varying snowmelt on subsurface flow in a mountain watershed: 1. Snowmelt simulation. *J. Hydr. Sc.*, **39**, 507-519.

Flerchinger, G.N. and K.E. Saxton, 1989: Simultaneous Heat and Water Model of a Freezing Snow-Residue-Soil System I. Theory and Development. *Trans. of the ASAE*, **32**, 565-571.

Gel'fan, A.N., 1989: Comparison of two methods of calculating soil freezing depth. *Soviet Met. and Hydrol.*, **2** 78-83.

Gusev, E.M., 1985: Approximate numerical calculation of soil freezing depth. *Sov. Meteorol. Hydrol.* **9**, 79-85.

Gusev, E.M. and. Nasonova, O.N., 1997: Modelling annual dynamics of soil water storage for agro- and natural ecosystems of the steppe and forest-steppe zones on a local scale. *Agric. For. Meteorol.* **85**, 171-191.

Guttman, N.B. and R.G. Quayle, 1996: A Historical Perspective of U.S. Climate Divisions. *Bull. Amer. Meteor. Soc.*, **77**, 293-303.

Hanson, C.L., Burton, D.P. and M. Molnau, 1988: *Soil Frost Distribution and Occurrence on a Mountainous Rangeland Watershed in Southwest Idaho*. Idaho Agricultural Experiment Station, 31 pp.

Harlan, R.L., 1973: Analysis of a coupled heat-fluid transport in partially frozen soil. *Water Resour. Res.* **9**, 1314-1323.

Jansson, P.E., 1991: *Soil Water and Heat Model Technical Description*. Rep. 165, Dept. of Soil Sci., Swedish Univ. Agric. Sci., Uppsala Sweden 72 pp.

Kennedy, I. and B. Sharratt, 1998: Model comparisons to simulate soil frost depth. *Soil Science*, **163**, 636-645.

Molnau, M. and Bissell, V.C., 1983: A continuous frozen ground index for flood forecasting. Proceedings of the Western Snow Conference, Vancouver WA, 109-119.

Palmer, W.C., 1965: *Meteorological Drought*. U.S. Department of Commerce, 58 pp.

Palmer, W.C. and A.V. Havens, 1958: A Graphical Technique for Determining Evapotranspiration by the Thornthwaite Method, *Mon. Wea. Rev.*, **86**, 123-128.

Ricard, J.A., Tobiasson, W. and A. Greatorex, 1976: *Technical Note: The Field Assembled Frost Gage*. U. S. Army Corps of Engineers/CRREL, 8 pp.

Rosenberg, N.J., 1974: *Microclimate: The Biological Environment*. John Wiley & Sons, 315 pp.

Sellers, W.D., 1965: *Physical Climatology*. The University of Chicago Press, 272 pp.

Sowers, G.F., 1979: *Introductory Soil Mechanics and Foundations: Geotechnical Engineering*, 4th Ed., Macmillan, New York, 621 pp.

Steurer, P.M. and J. Crandell, 1995: Comparison of the methods used to create an estimate of the air-freezing index. *Cold Regions Science and Technology*, **9** 64-74.

Thornthwaite, C. W., 1948: An Approach Toward Rational Classification of Climate. *Geog. Rev.*, **38**, 55-94.

USDA, 1941: *Climate and Man, Yearbook of Agriculture 1941,* Washington, U.S. Government Printing Office, 1248 pp.

van Es, H.M., A.T DeGaetano and D.S. Wilks, 1998: Space-time upscaling of plot-based research information: frost tillage, *Nutrient Cycling in Agroecosystems*, 50, 85-90.

TABLE 1. Meteorological and site characteristic input required by the SHAW model.

Weather Data	Site Characteristics
Air temperature	Slope
Wind speed	Aspect
Initial snow depth	Latitude
Initial snow density	Roughness parameters
Humidity	Albedo
Precipitation	Leaf area index
Solar radiation	Plant height
	Rooting depths
Soil Data	**Residue Parameters**
Initial soil temperature	Residue loading
Initial soil moisture	Residue layer thickness
Bulk density	Percent coverage
Saturated hydraulic conductivity	Albedo
Saturated thermal conductivity	
Albedo	

TABLE 2. Change in maximum frost depth during two seasons associated with 20 and 50% changes (increases and decreases) in the empirical coefficients used by Campbell (1985) and θ, φ_m and ϕ, expressed as a percentage of the altered to unaltered frost depths. Unaltered frost depths of 17.7 and 73.9 cm were indicated during the 1977-78 and 1978-79 seasons, respectively.

1977– 1978

	INCREASE		DECREASE	
PARAMETER	50%	20%	20%	50%
A	111	105	95	86
B	102	101	99	98
C	116	109	89	79
D	103	101	99	98
E	97	99	101	103
θ	106	103	95	94
φ_m	91	96	104	111
ϕ	70	87	112	129
1978–1979				
A	116	106	93	81
B	105	102	97	94
C	100	100	100	90
D	100	100	100	100
E	100	100	100	99
θ	104	96	105	105
φ_m	97	99	101	102
ϕ	73	88	118	156

FIGURE CAPTIONS

Figure 1. Schematic diagram showing the NRCC model's frozen soil state. Heat fluxes through the centers of each layer are indicated by the bold arrows. The stippled area represents the change in energy storage ΔQ_L and the hatched areas represent ΔQ_U.

Figure 2. Maximum soil freezing depths at Ithaca, New York based on SHAW model simulations with fixed 35% (black), 15% (shaded) and 5% (hatched) water contents.

Figure 3. Observed and simulated soil freezing depths at Reynolds Creek, Idaho during the winter of 1977-78. The sold black curve shows the modeled frost depth using the revised NRCC model. Surface thaw depths (i.e. the depth of unfrozen soil above the buried frozen layer) are indicated by the dotted black line. Frost depths obtained using the original NRCC model are shown by the dashed line. Observed frost depths are shown by the Xs.

Figure 4. As in Figure 3, but for the winter of 1978-79. Snow depth is given by the solid gray line.

Figure 5. Observed (light) and modeled (dark) maximum seasonal frost depths at Reynolds Mountain and Lower Sheep Creek, Idaho. No soil freezing was observed or estimated during 1983-84 at Reynolds Mountain.

Figure 6. Observed versus soil temperature-inferred soil freezing depths at Lind, Washington during 1994-95. Model simulated soil freezing levels are indicated by the solid black line and surface thaw depths by the dashed line. The shaded area represents the ± 1°C position of the 0°C isotherm (dotted line). Snow depth is given by the solid gray line.

Figure 7. As in Figure 6, but for Mandan, North Dakota during 1996-97.

Figure 8. Modeled versus measured soil freezing depths at DeKalb, Illinois during the winter of 1998-99. Modeled frost depths are given by the solid black line, with surface thawing indicated by the dashed line. Soil freezing observations are indicated by the black dots which represent the median of three frost tube observations. The thin line through each dot gives the range of observations. Snow depth is indicated by the gray line.

Figure 9. Collective scatterplot of observed (solid symbols) and interpolated (open symbols) versus modeled maximum frost depths for 32 verification sites. Reynolds Creek watershed data are shown by circles, SCAN sites and frost tube observations are indicated by squares.

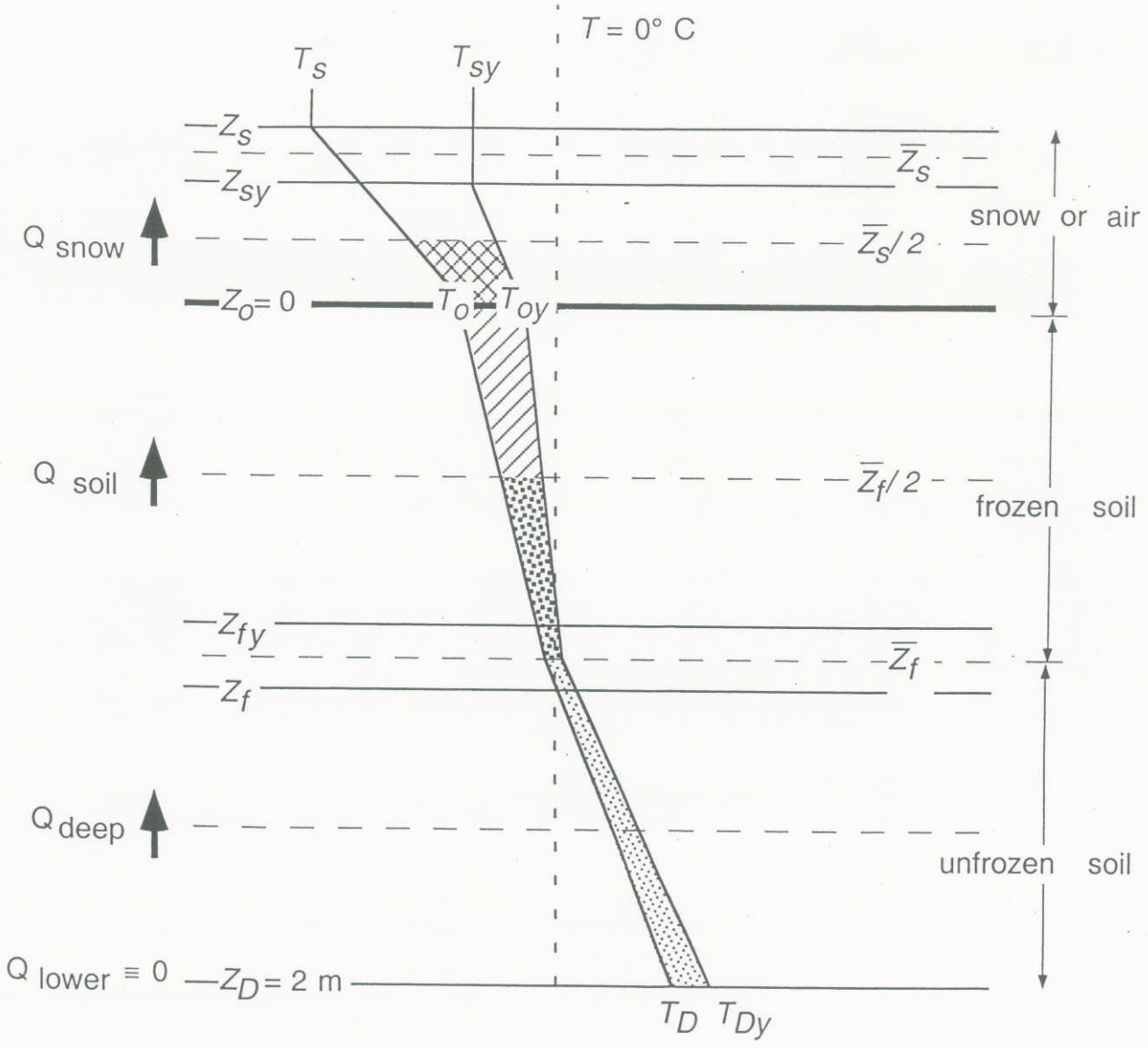

Figure 1. Schematic diagram showing the NRCC model's frozen soil state. Depths below or above (in the case of snow and/or air) the surface are indicated by Z and temperatures are indicated by T. Subscripts indicate snow (s), the soil surface (0), frozen soil (f), and the lower boundary (D). The subscript "y" refers to the value observed or estimated for the previous day. Heat fluxes through the centers of each layer are indicated by the bold arrows. The stippled area represents the change in energy storage ΔQ_L and the hatched areas represent ΔQ_U.

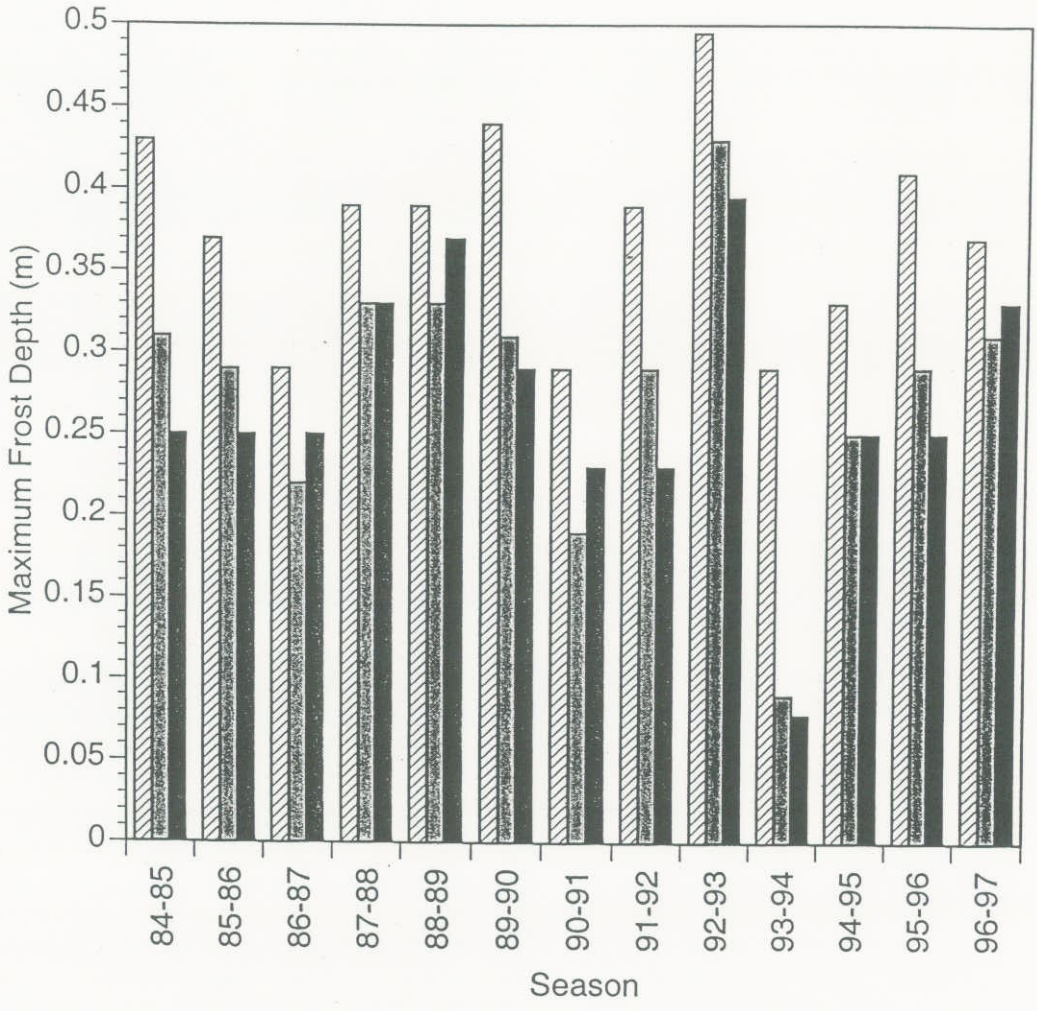

Figure 2. Maximum soil freezing depths at Ithaca, New York based on SHAW model simulations with fixed 35% (black), 15% (shaded) and 5% (hatched) water contents.

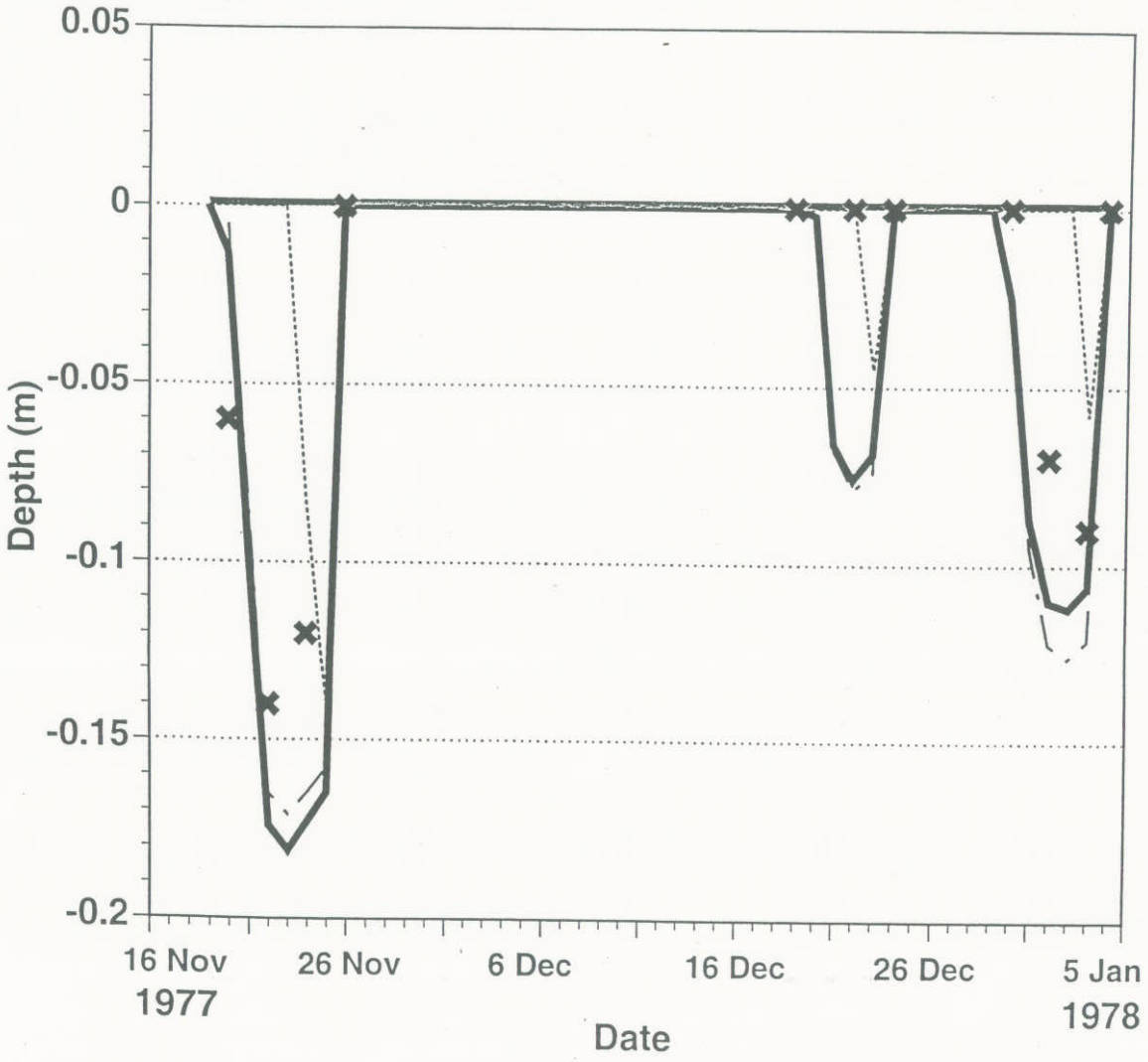

Figure 3. Observed and simulated soil freezing depths at Reynolds Creek, Idaho during the winter of 1977-78. The solid black curve shows the modelled frost depth using the revised NRCC model. Surface thaw depths are indicated by the dotted black line. Frost depths obtained using the orginal NRCC model are shown by the dashed line. Snow depth is given by the gray line. Observed frost depths are shown by the Xs.

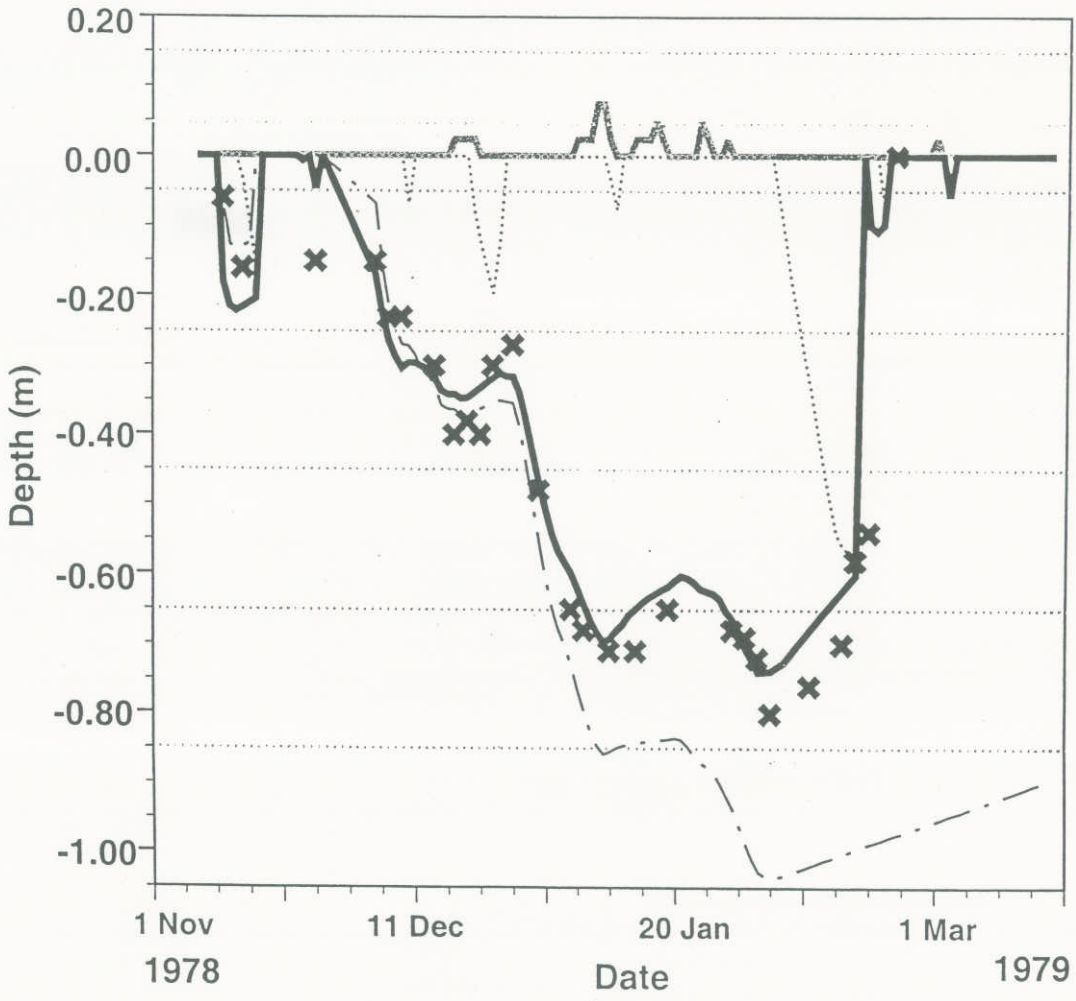

Figure 4. As in Figure 3, but for the winter of 1978-79.

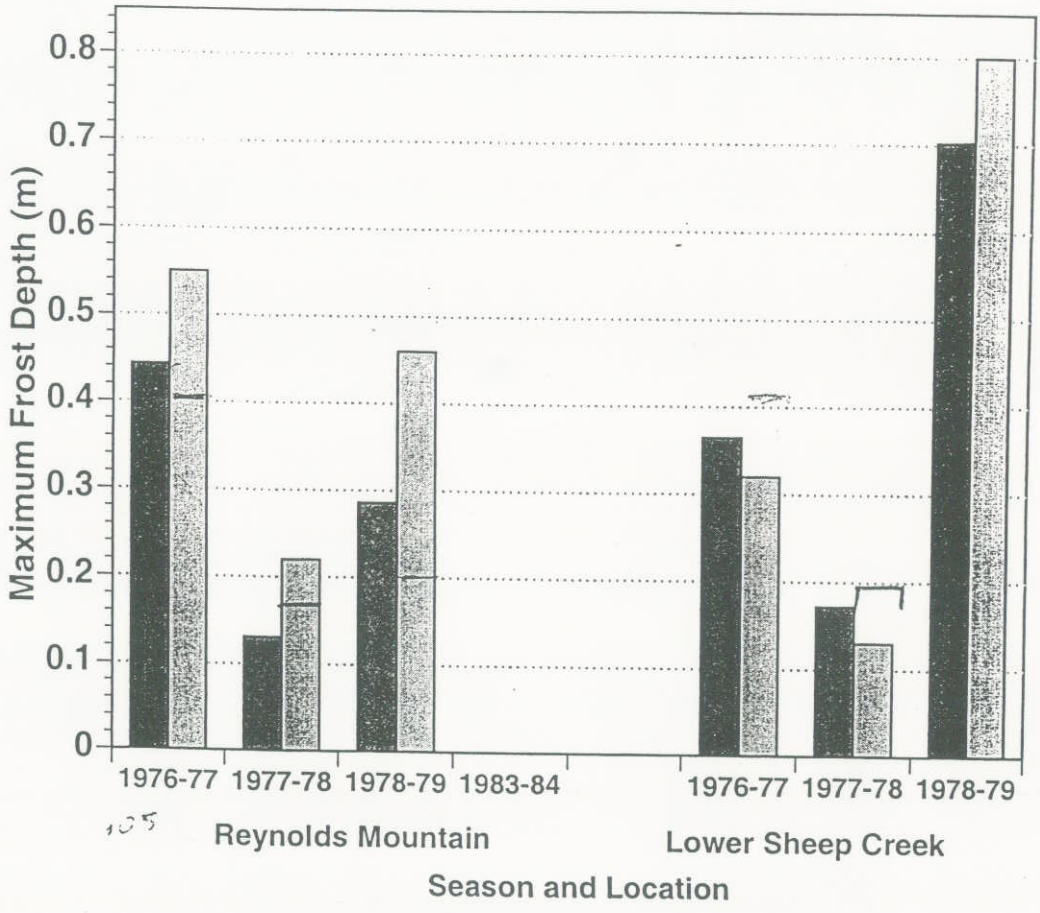

Figure 5. Observed (light) and modelled (dark) maximum seasonal frost depths at Reynolds Mountain and Lower Sheep Creek, Idaho. No soil freezing was observed or estimated during 1983-84 at Reynolds Mountain.

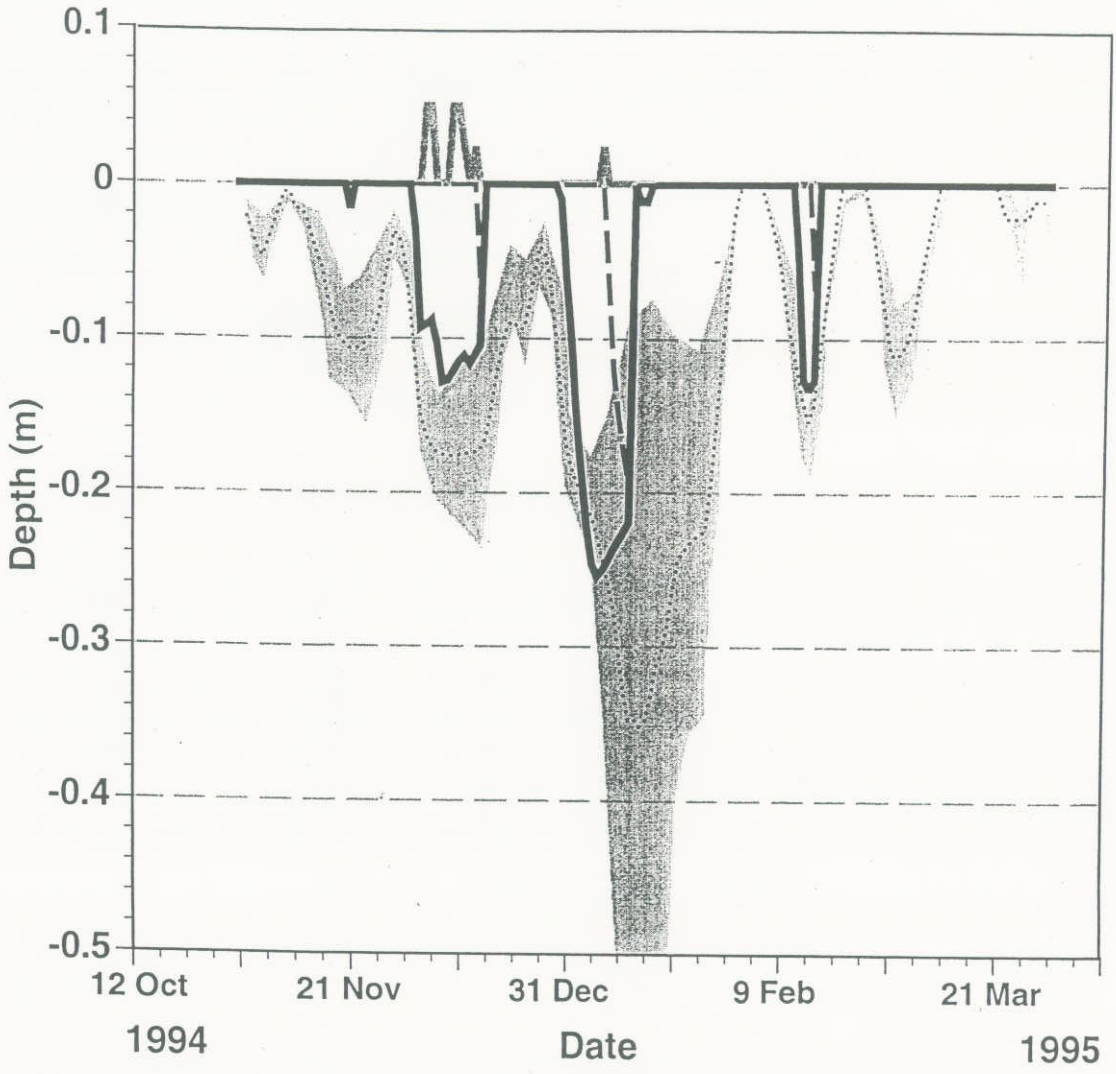

Figure 6. Observed versus soil temperature-infered soil freezing depths at Lind, Washington during 1994-95. Model simulated soil freezing levels are indicated by the solid black line and surface thaw depths by the dashed line. The shaded area represents the ± 1°C position of the 0°C isotherm (dotted line). Snow depth is given by the solid gray line.

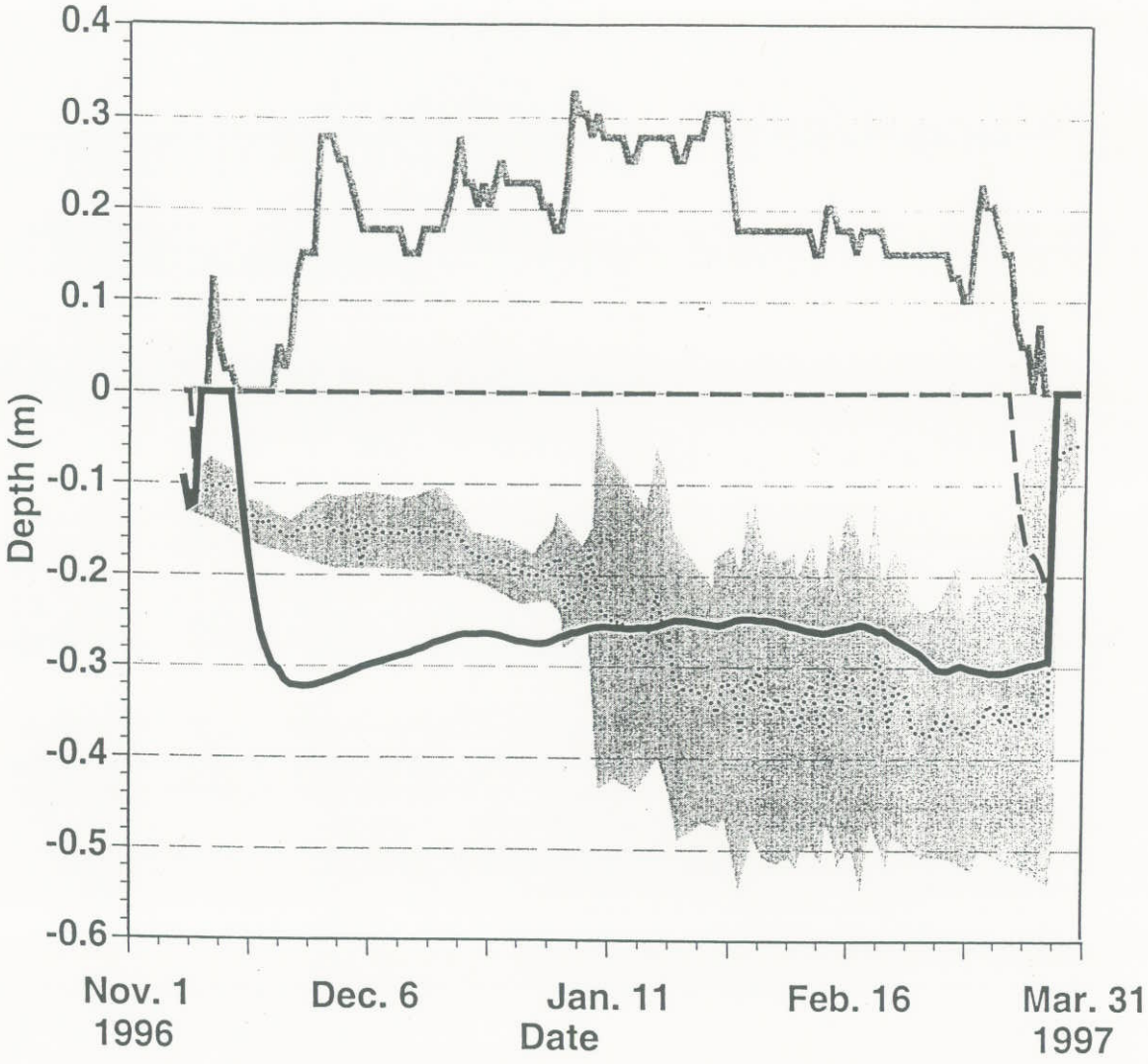

Figure 7. As in Figure 6, but for Mandan, North Dakota during 1996 - 97.

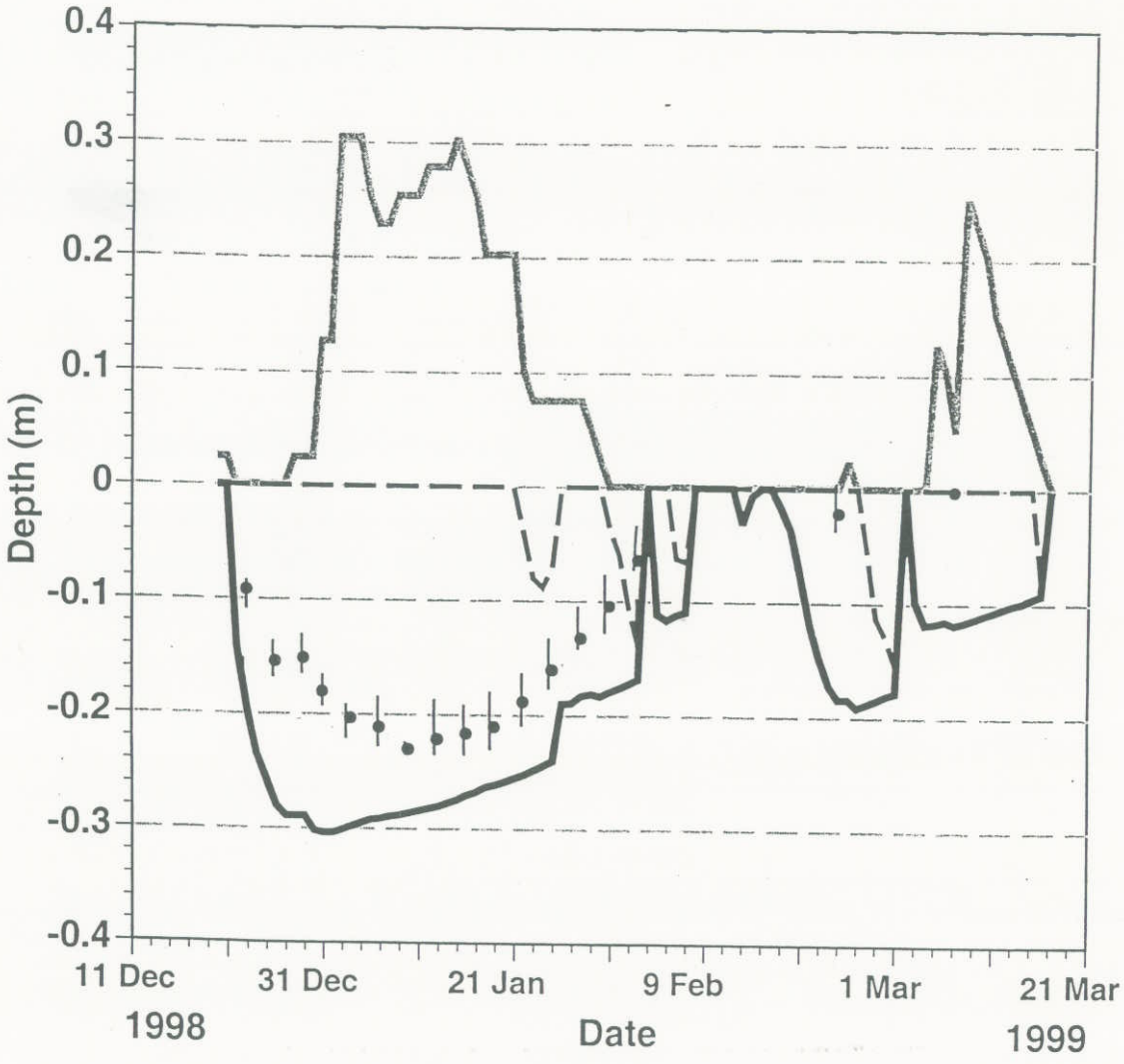

Figure 8. Modelled versus measured soil freezing depths at DeKalb, Illinois during the winter of 1998-99. Modelled frost depths are given by the solid black line, with surface thawing indicated by the dashed line. Soil freezing observations are indicated by the black dots which represent the median of three frost tube observations. The thin line through each dot gives the range of observations. Snow depth is indicated by the gray line.

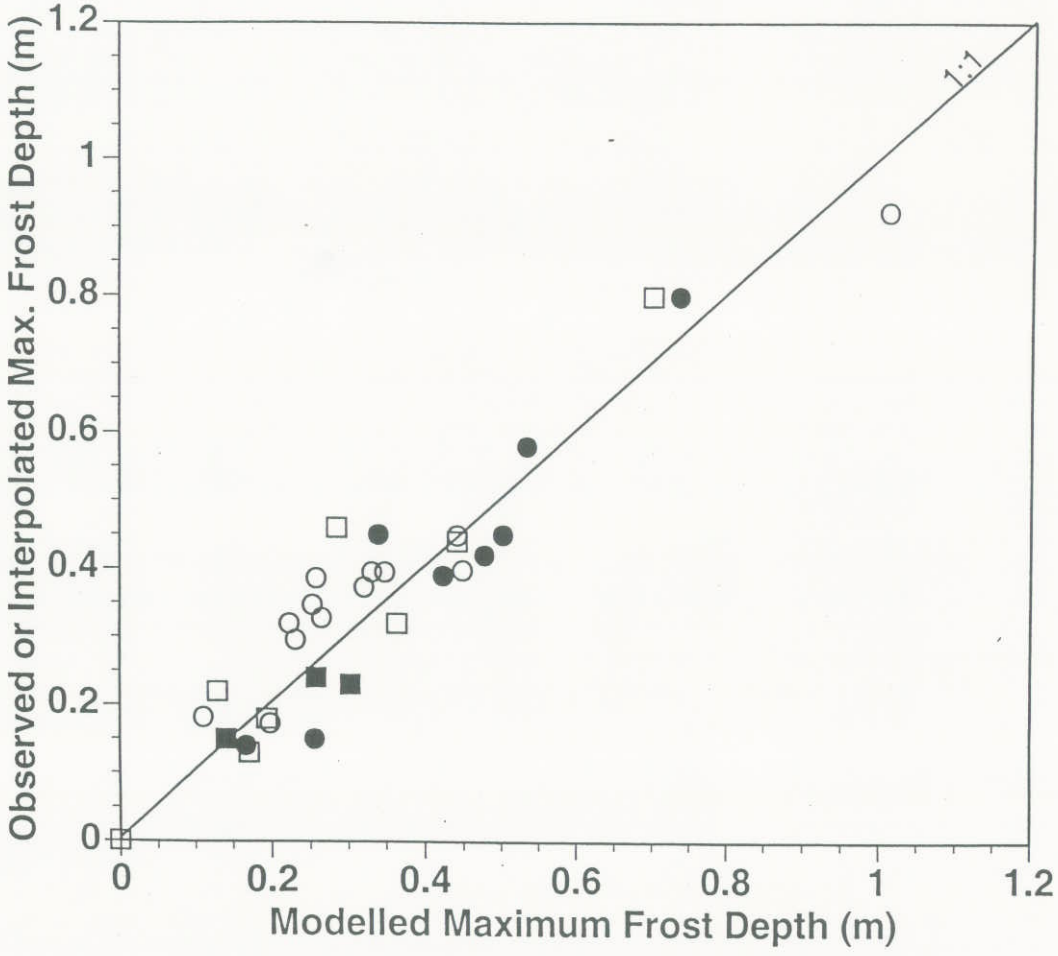

Figure 9. Collective scatterplot of observed (solid symbols) and interpolated (open symbols) versus modelled maximum frost depths for 32 verification sites. Reynolds Creek watershed data are shown by circles, SCAN sites and frost tube observations are indicated by squares.

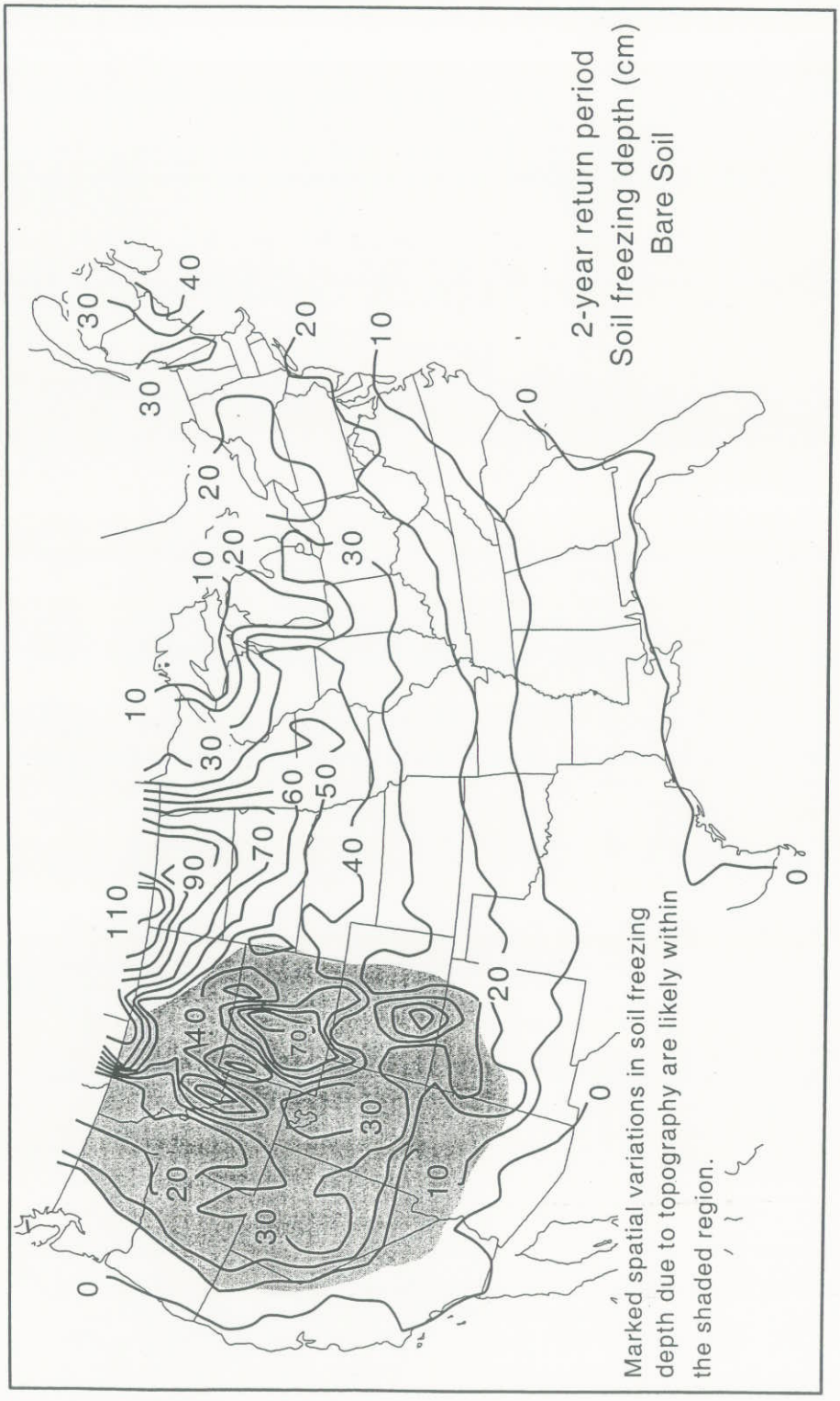
2-year return period
Soil freezing depth (cm)
Bare Soil
Marked spatial variations in soil freezing depth due to topography are likely within the shaded region.

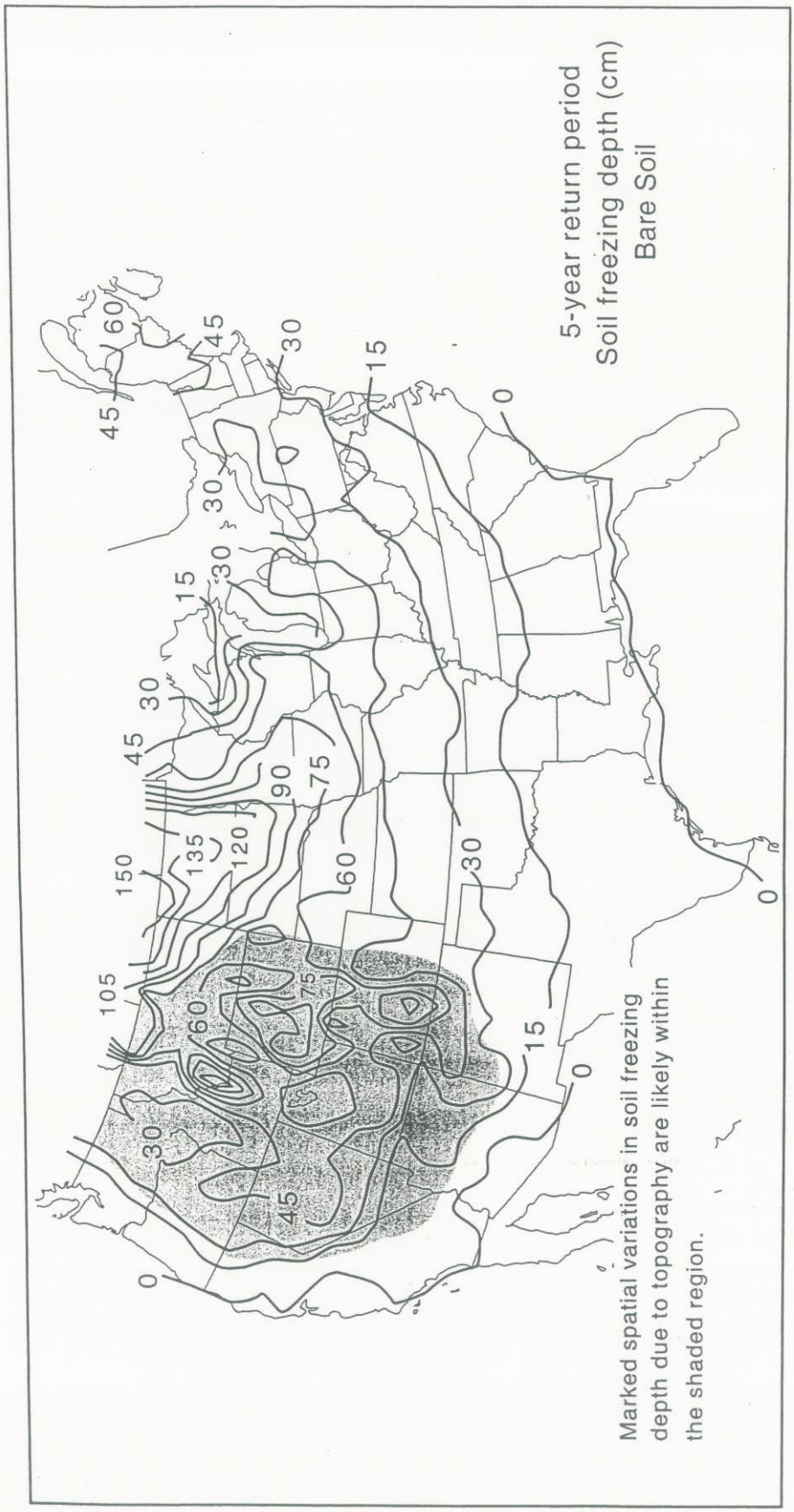
5-year return period
Soil freezing depth (cm)
Bare Soil
Marked spatial variations in soil freezing depth due to topography are likely within the shaded region.

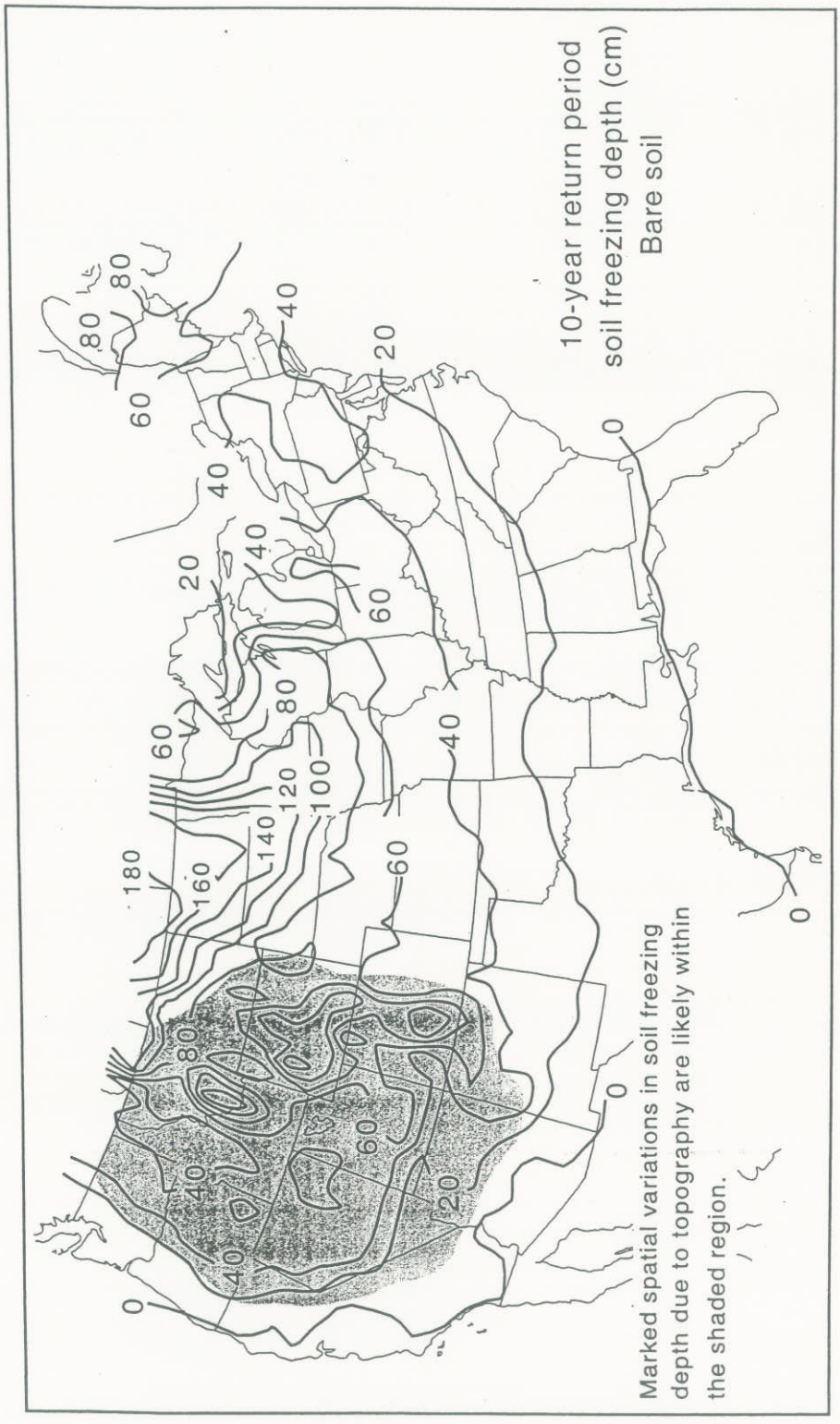
10-year return period
soil freezing depth (cm)
Bare soil
Marked spatial variations in soil freezing
depth due to topography are likely within
the shaded region.

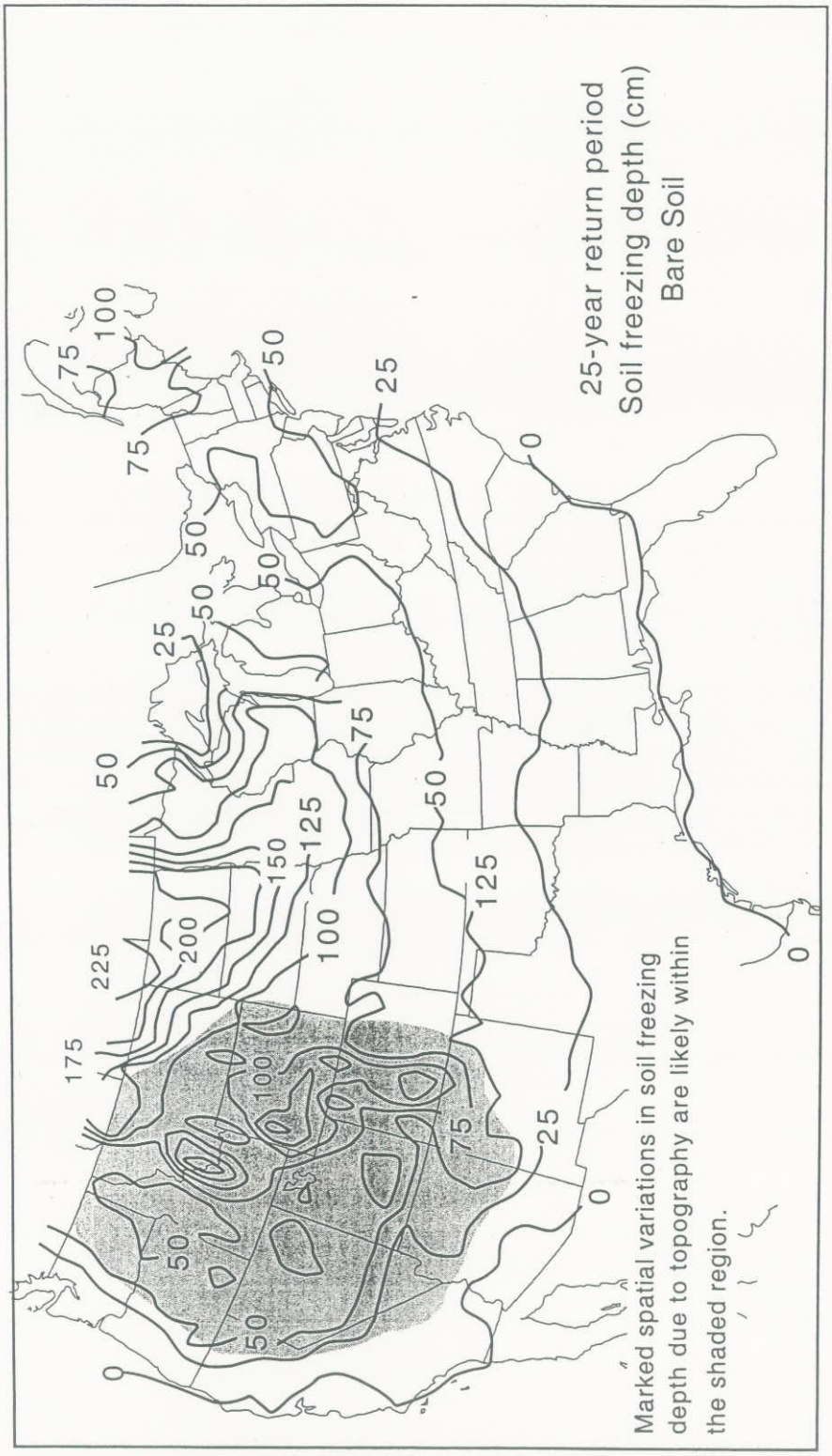
25-year return period
Soil freezing depth (cm)
Bare Soil
Marked spatial variations in soil freezing depth due to topography are likely within the shaded region.

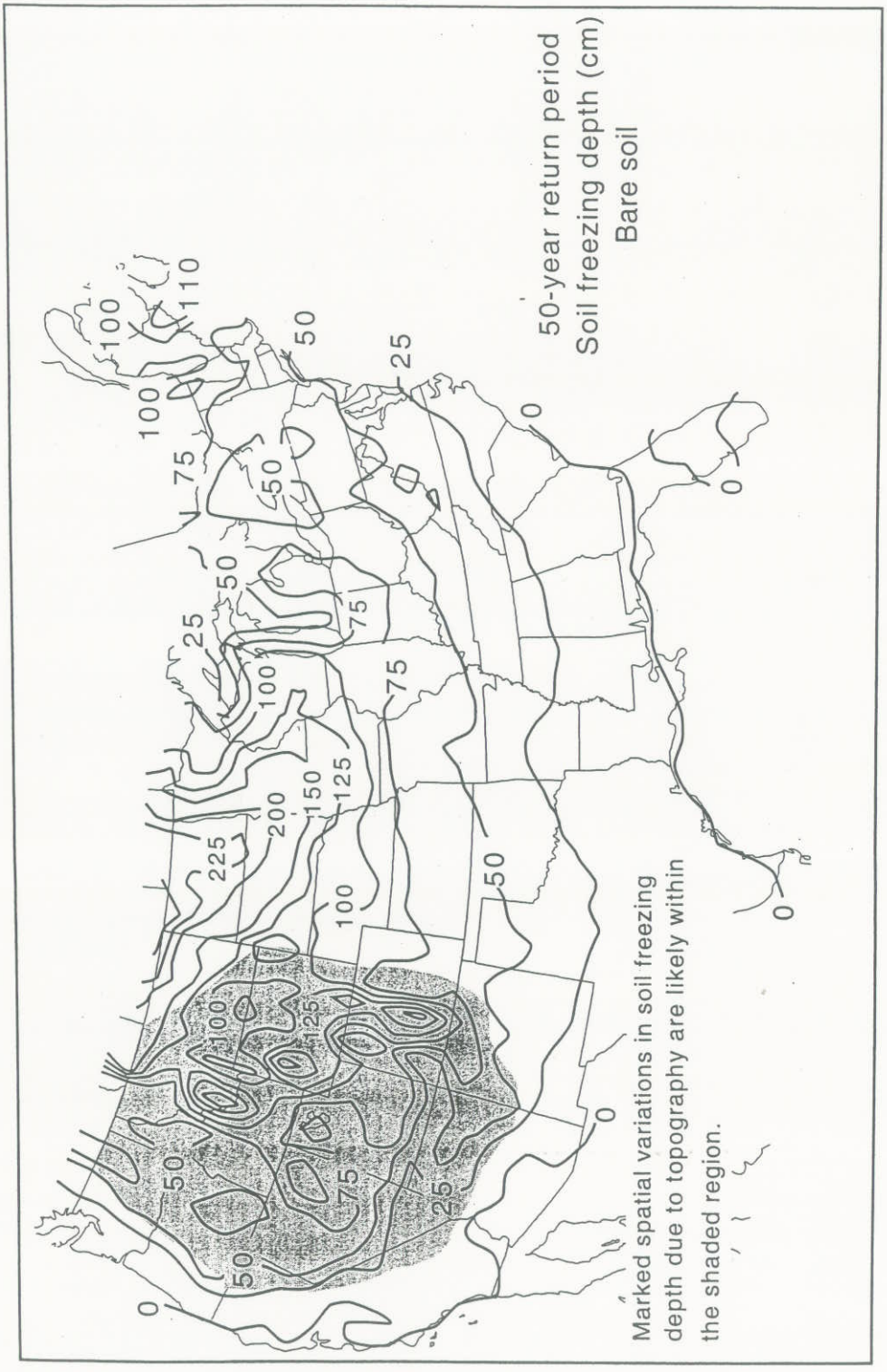
50-year return period
Soil freezing depth (cm)
Bare soil
Marked spatial variations in soil freezing depth due to topography are likely within the shaded region.

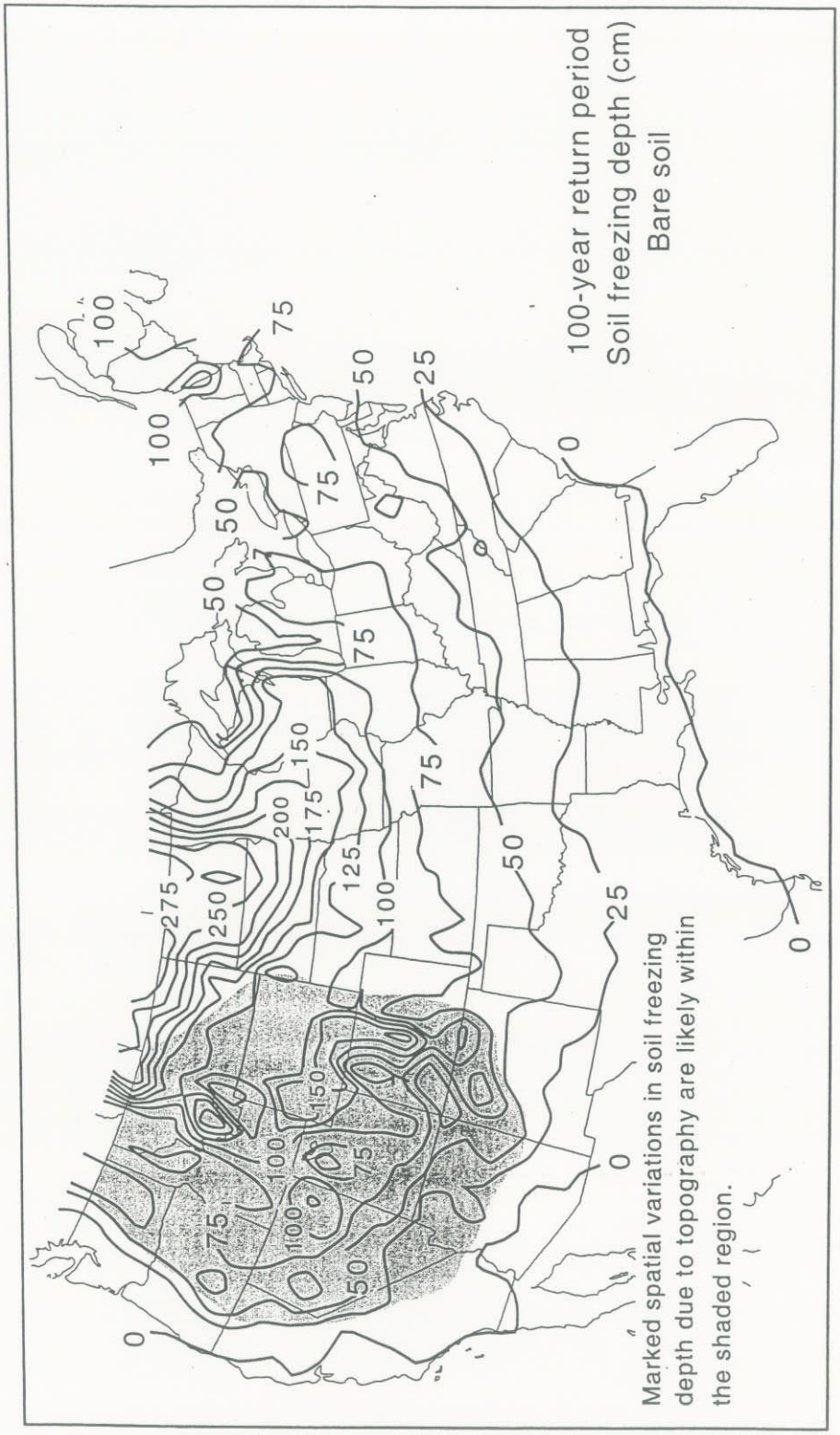
100-year return period
Soil freezing depth (cm)
Bare soil
Marked spatial variations in soil freezing depth due to topography are likely within the shaded region.

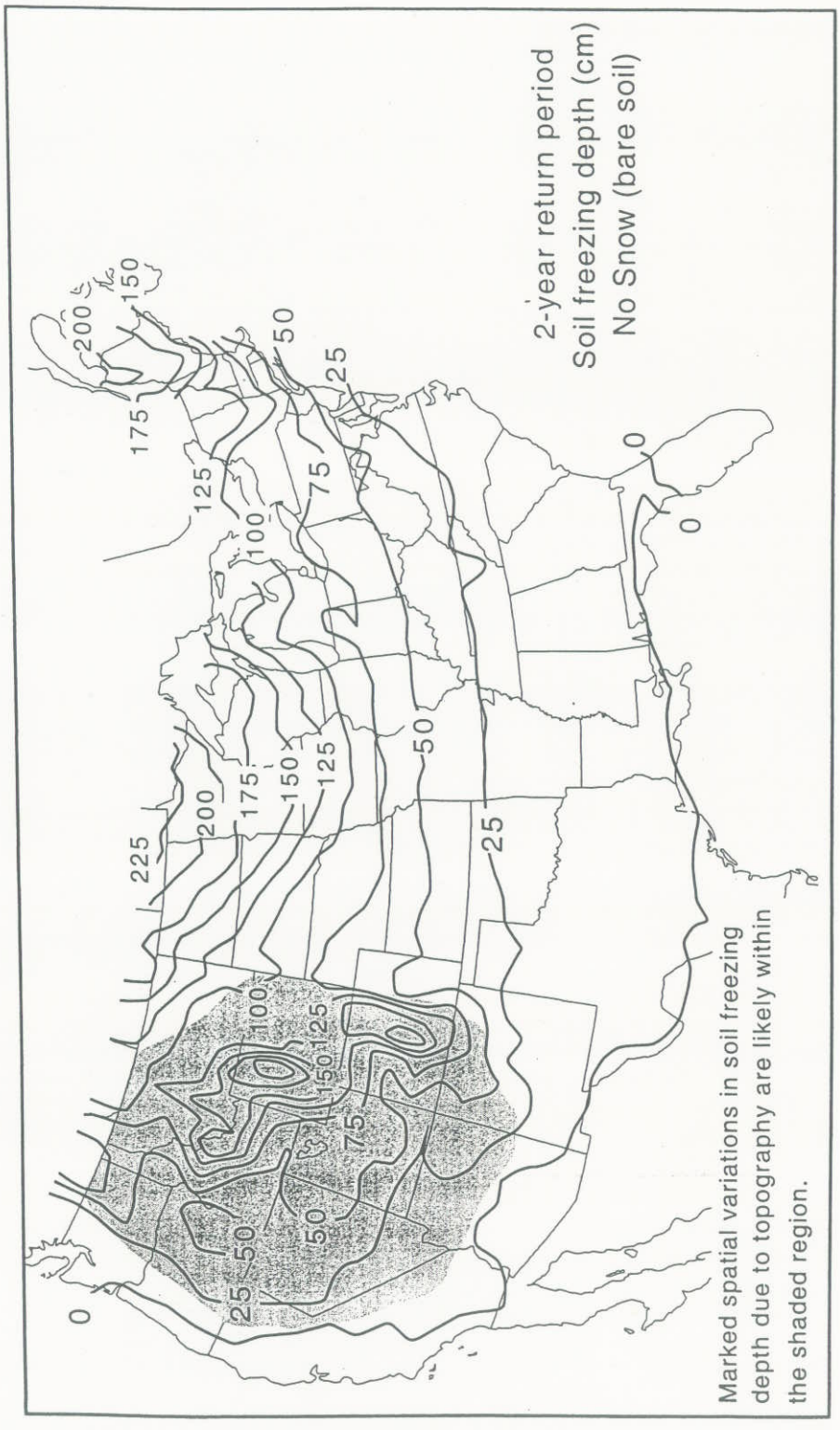
2-year return period
Soil freezing depth (cm)
No Snow (bare soil)
Marked spatial variations in soil freezing depth due to topography are likely within the shaded region.

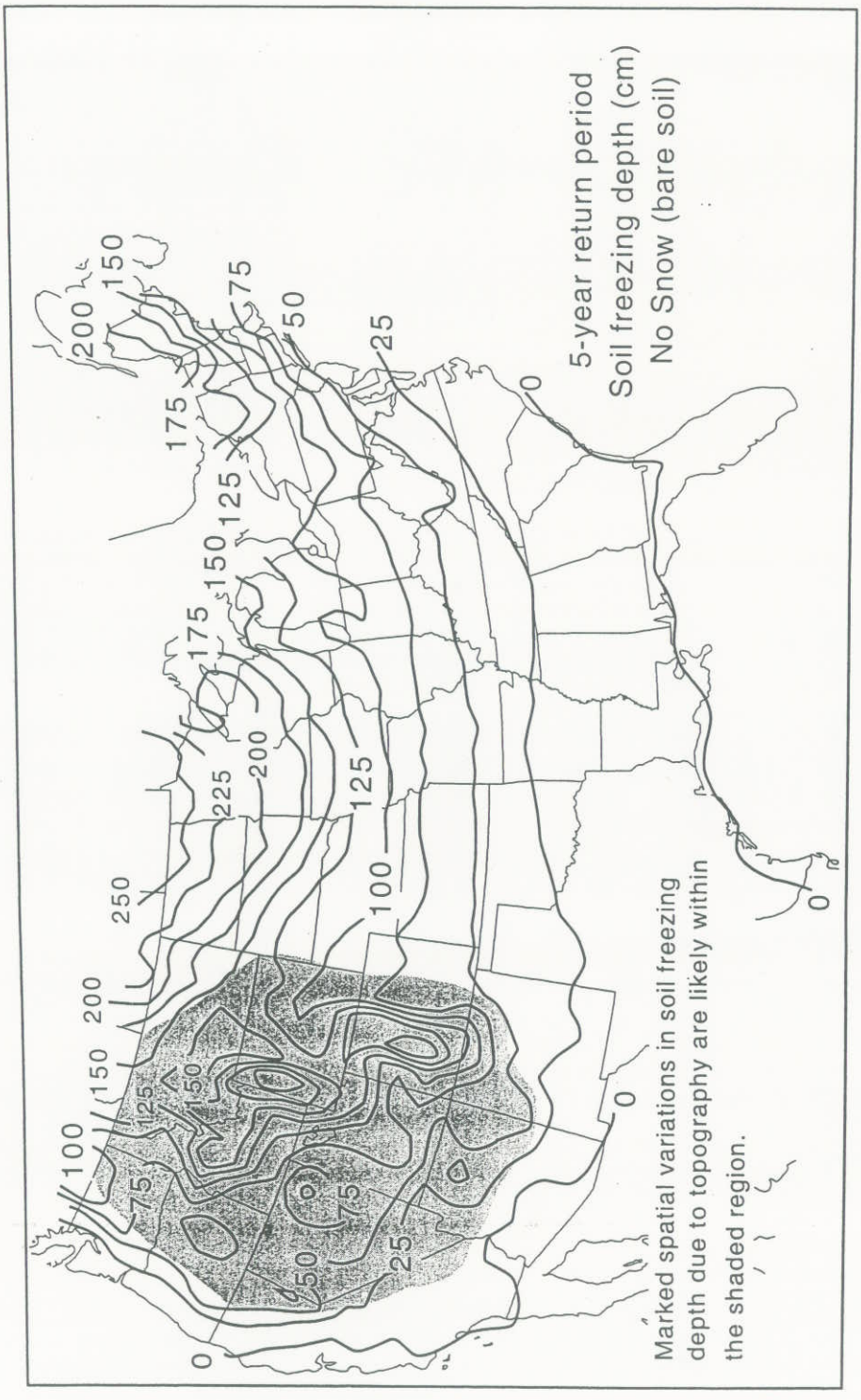
5-year return period
Soil freezing depth (cm)
No Snow (bare soil)
Marked spatial variations in soil freezing depth due to topography are likely within the shaded region.

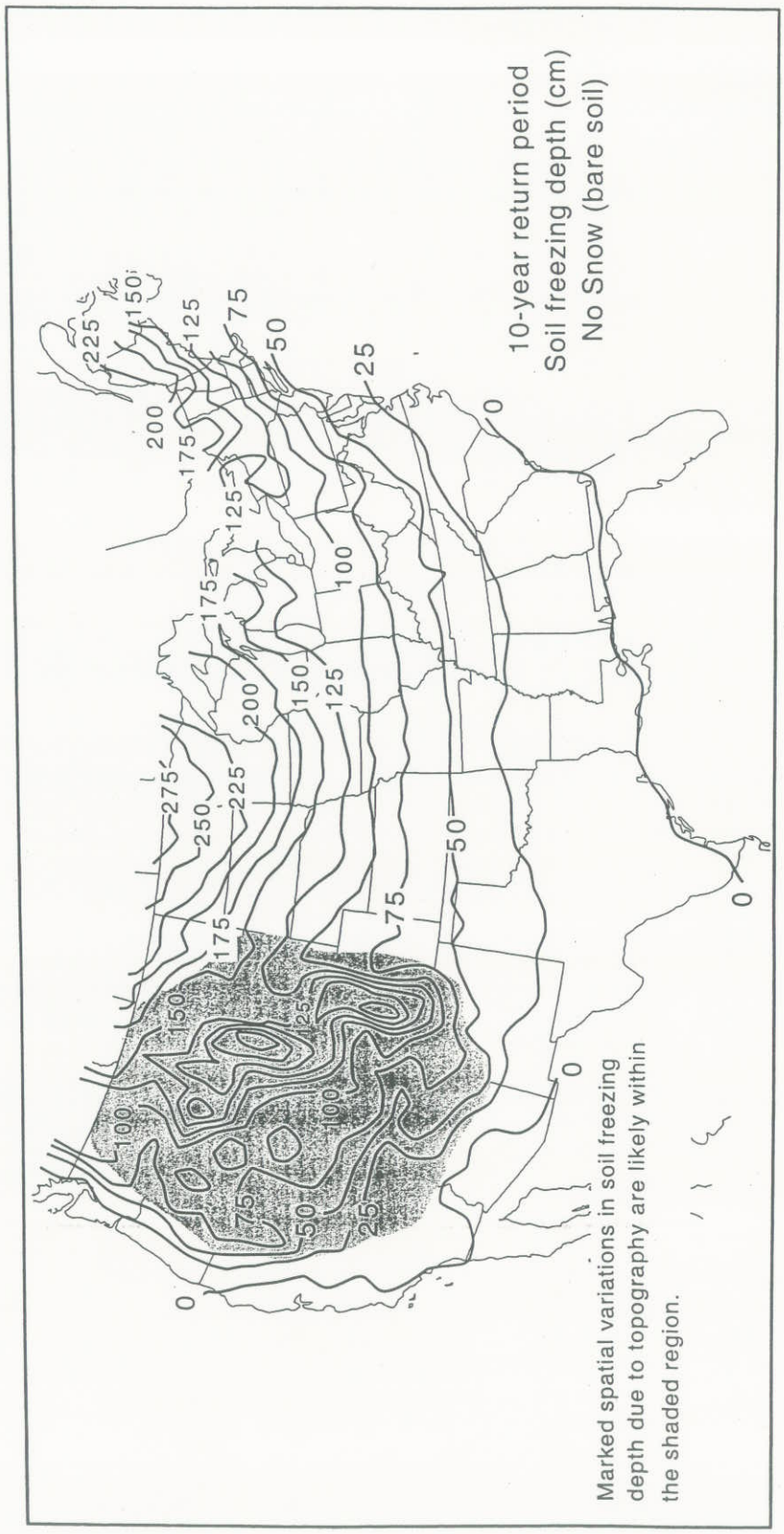
10-year return period
Soil freezing depth (cm)
No Snow (bare soil)
Marked spatial variations in soil freezing depth due to topography are likely within the shaded region.

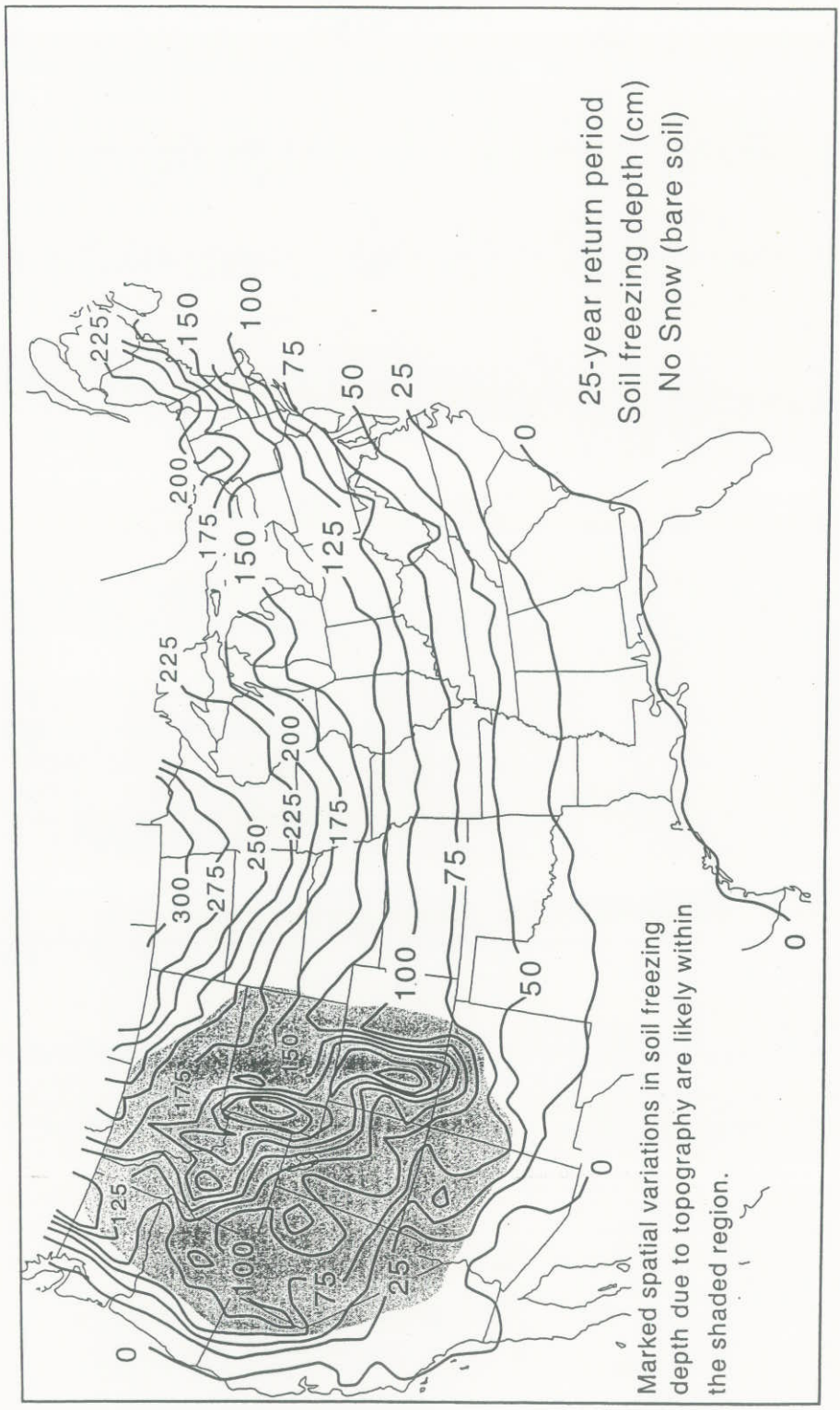
25-year return period
Soil freezing depth (cm)
No Snow (bare soil)
Marked spatial variations in soil freezing depth due to topography are likely within the shaded region.

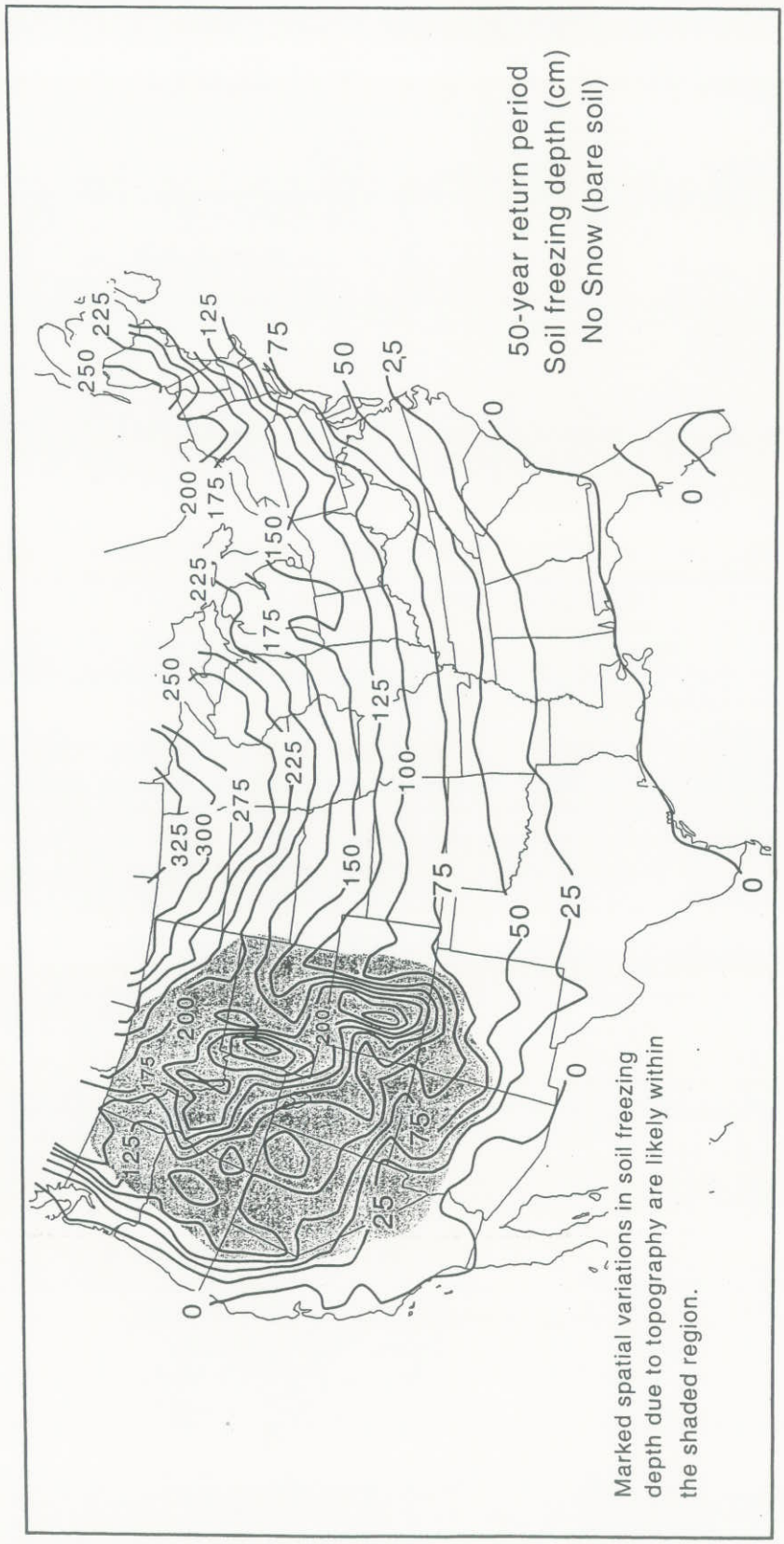
50-year return period
Soil freezing depth (cm)
No Snow (bare soil)
Marked spatial variations in soil freezing depth due to topography are likely within the shaded region.

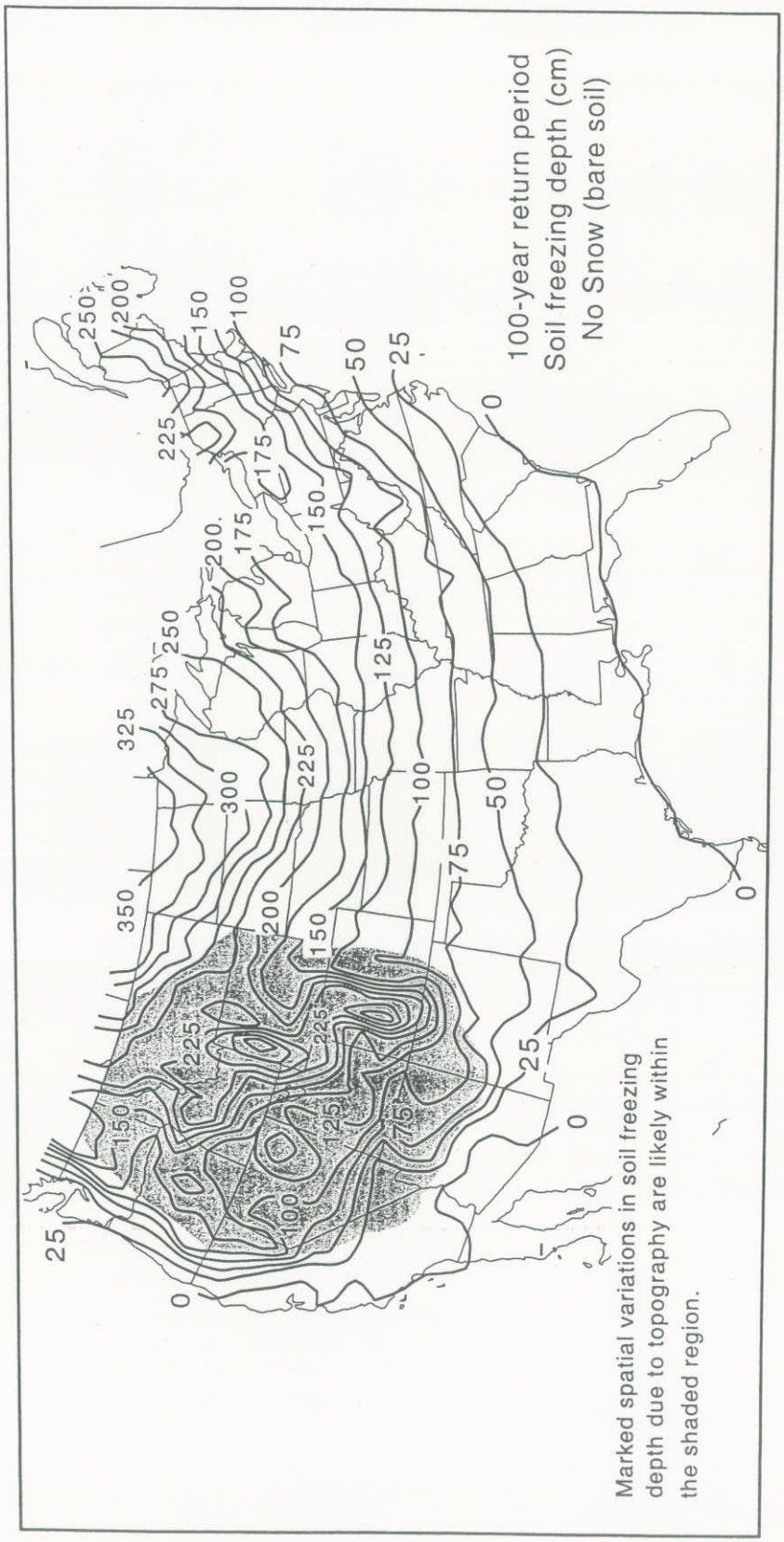
100-year return period
Soil freezing depth (cm)
No Snow (bare soil)
Marked spatial variations in soil freezing depth due to topography are likely within the shaded region.

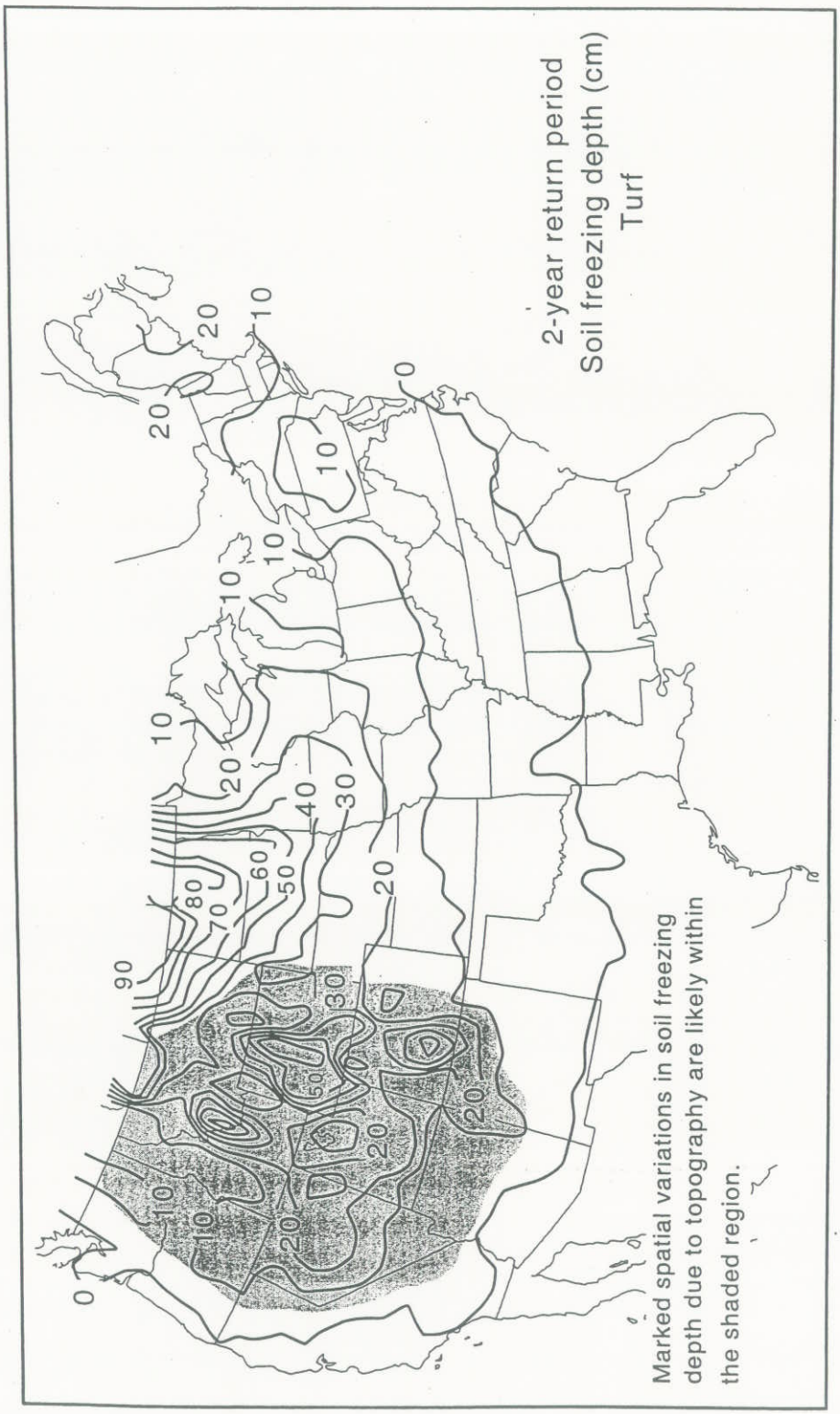
2-year return period
Soil freezing depth (cm)
Turf
Marked spatial variations in soil freezing depth due to topography are likely within the shaded region.

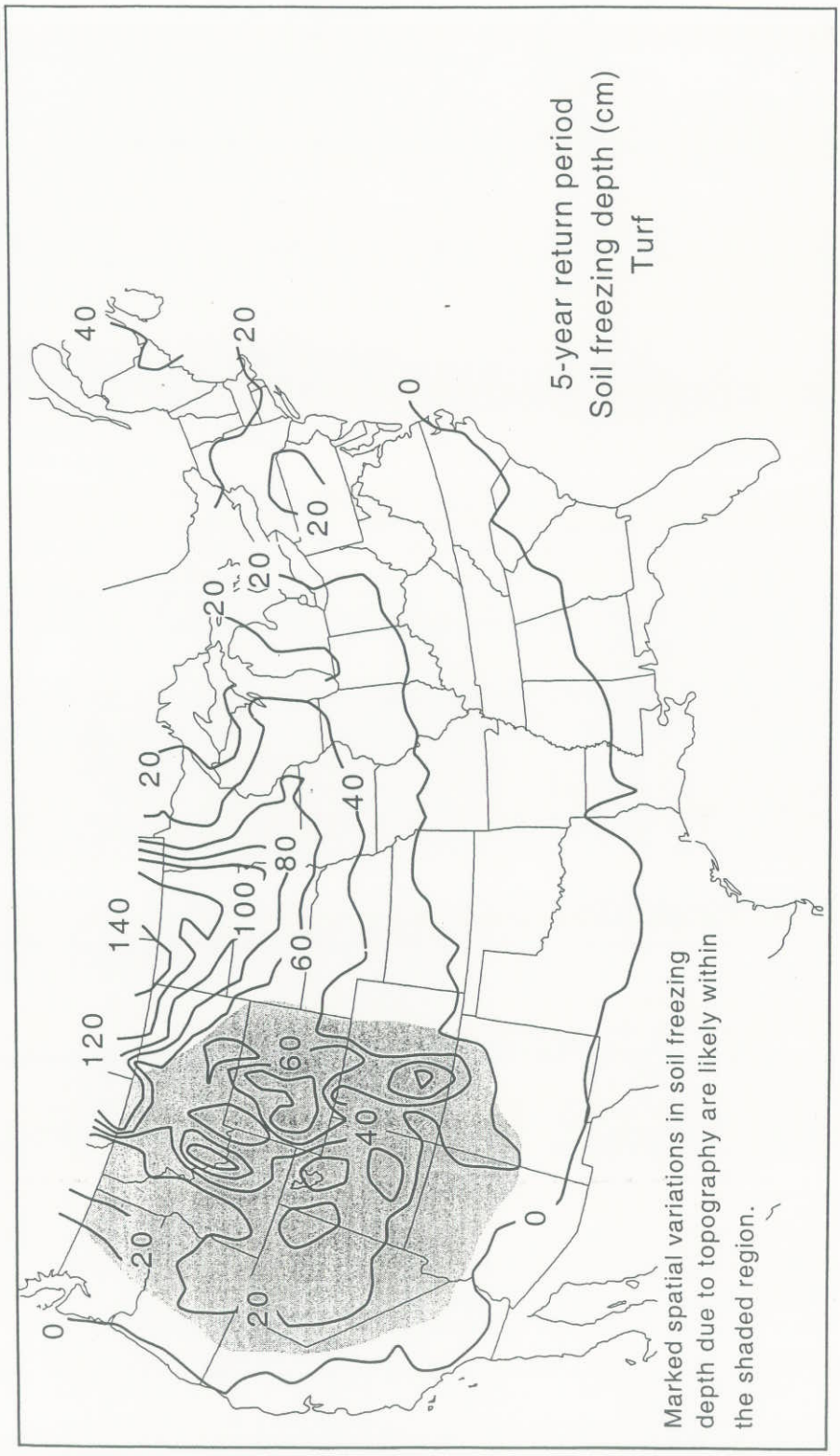
5-year return period
Soil freezing depth (cm)
Turf
Marked spatial variations in soil freezing depth due to topography are likely within the shaded region.
0
20
40
60
80
100
120
140

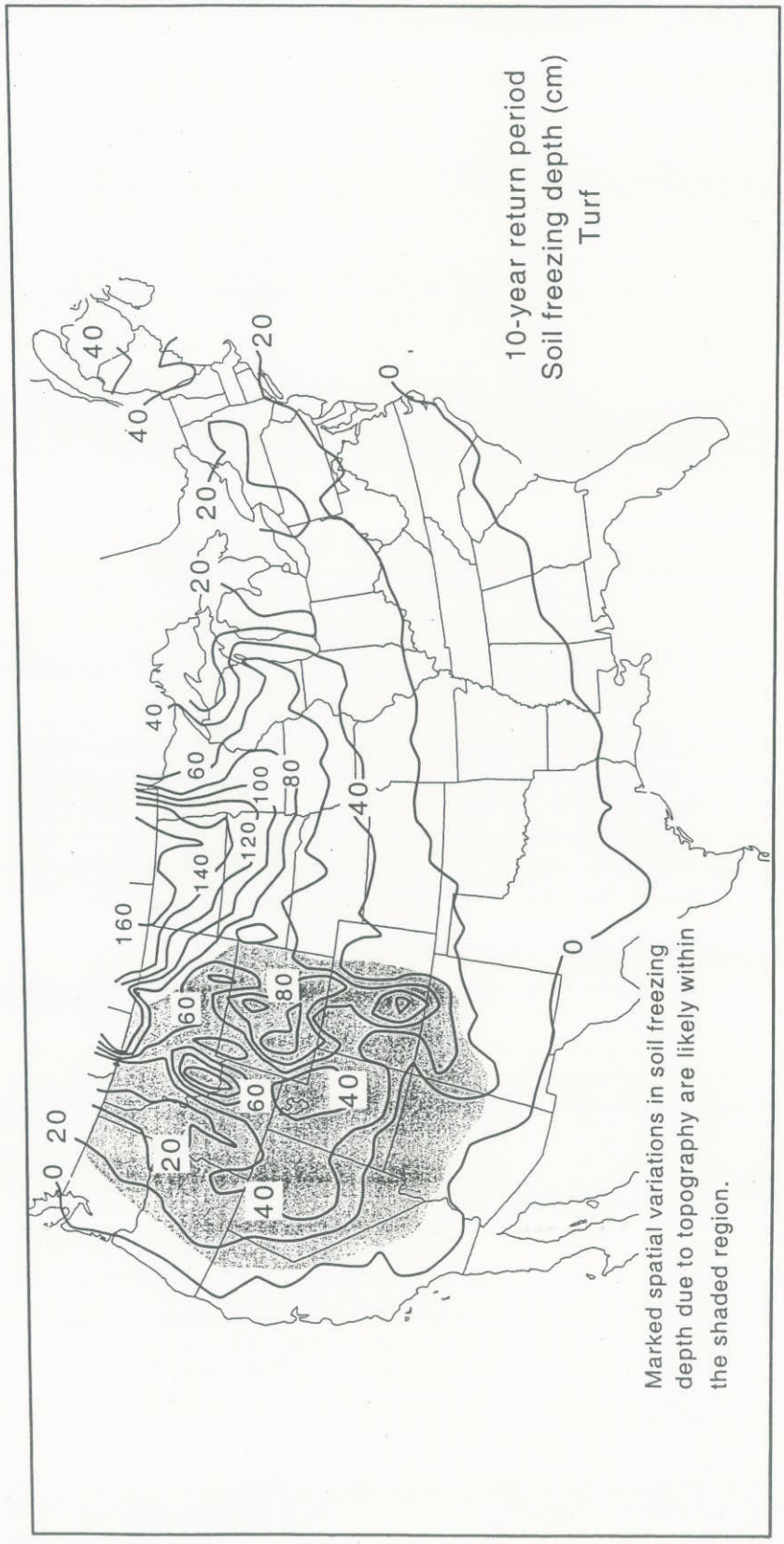
10-year return period
Soil freezing depth (cm)
Turf
Marked spatial variations in soil freezing depth due to topography are likely within the shaded region.

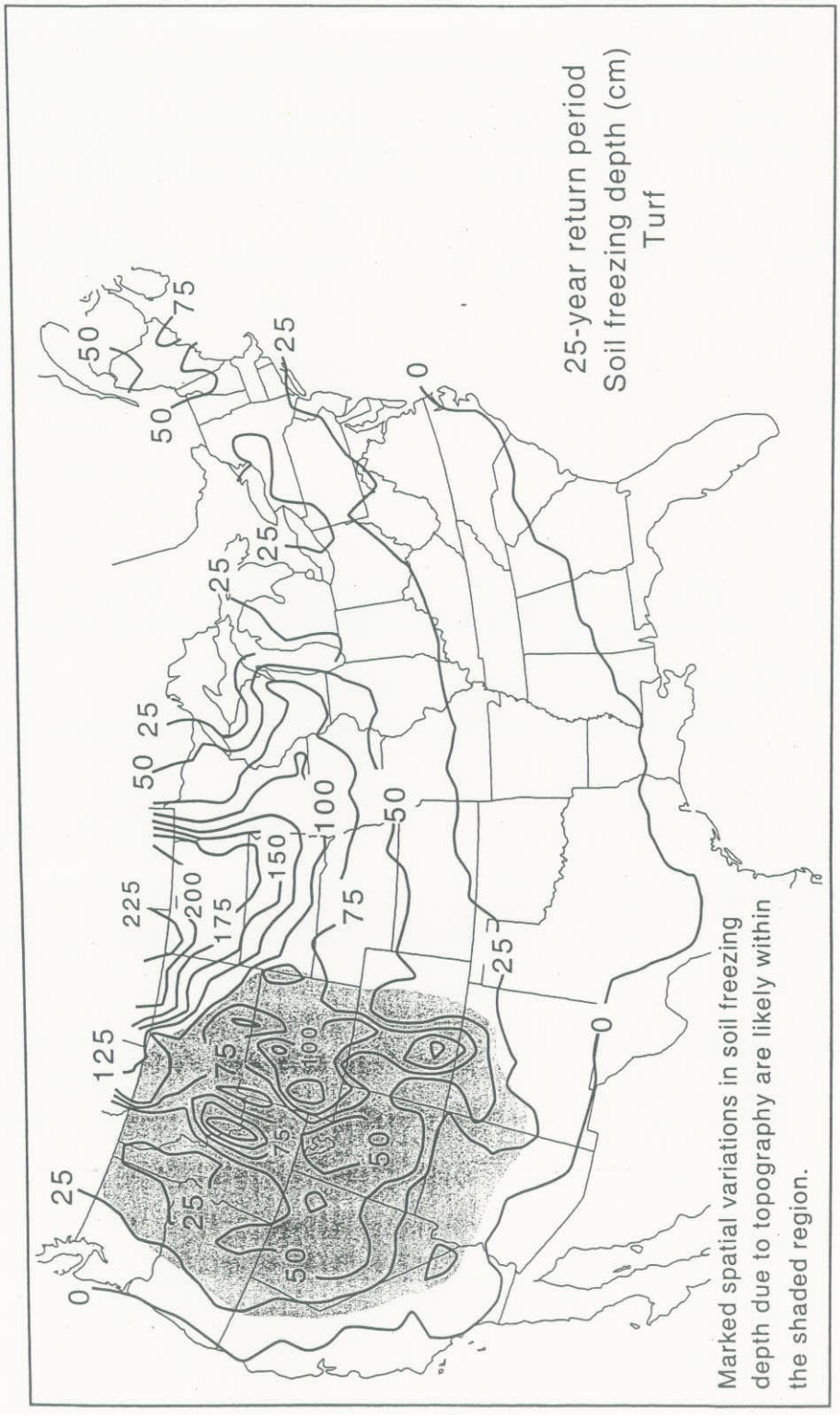
25-year return period
Soil freezing depth (cm)
Turf
Marked spatial variations in soil freezing depth due to topography are likely within the shaded region.

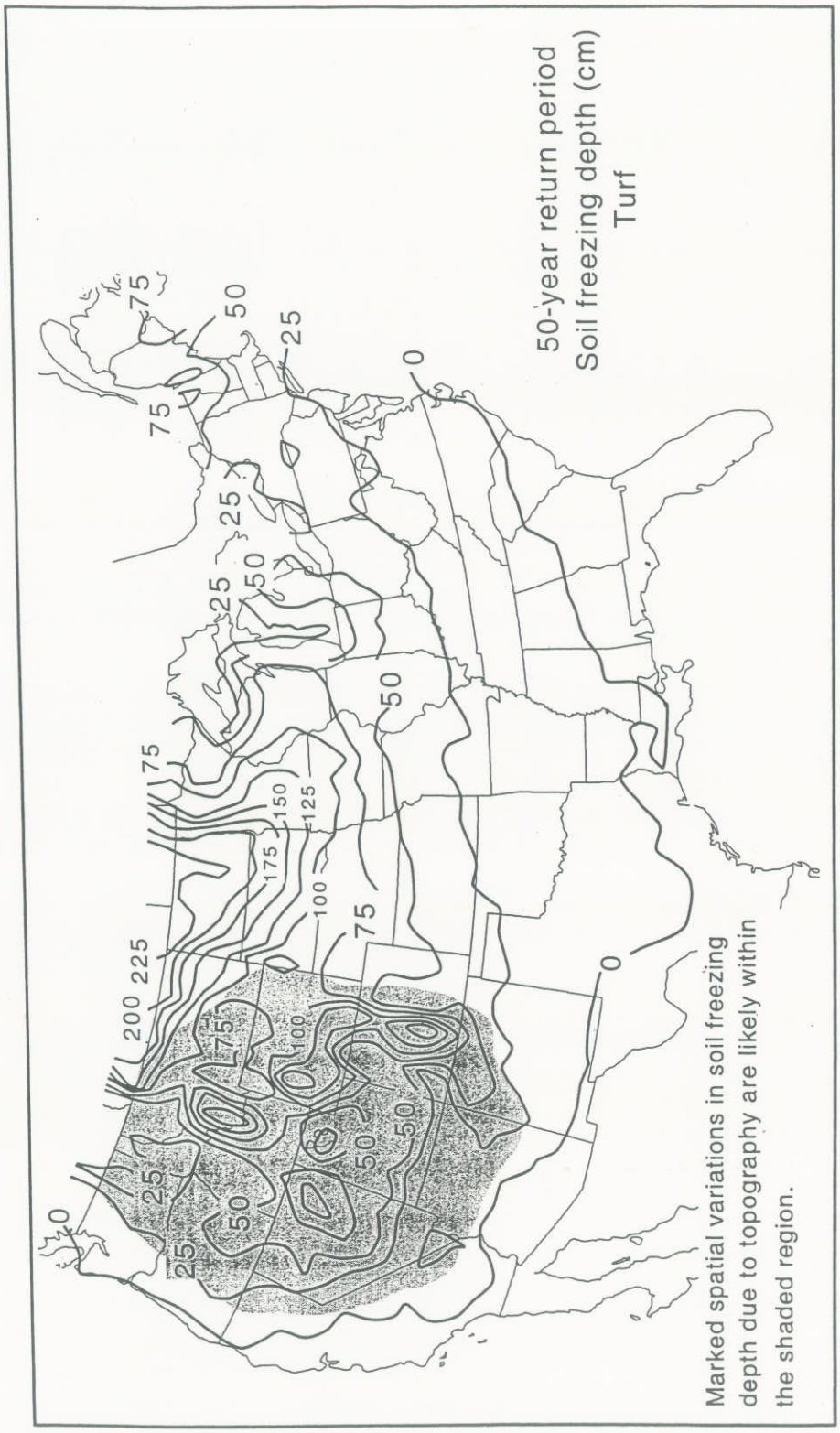
50-year return period
Soil freezing depth (cm)
Turf
Marked spatial variations in soil freezing depth due to topography are likely within the shaded region.

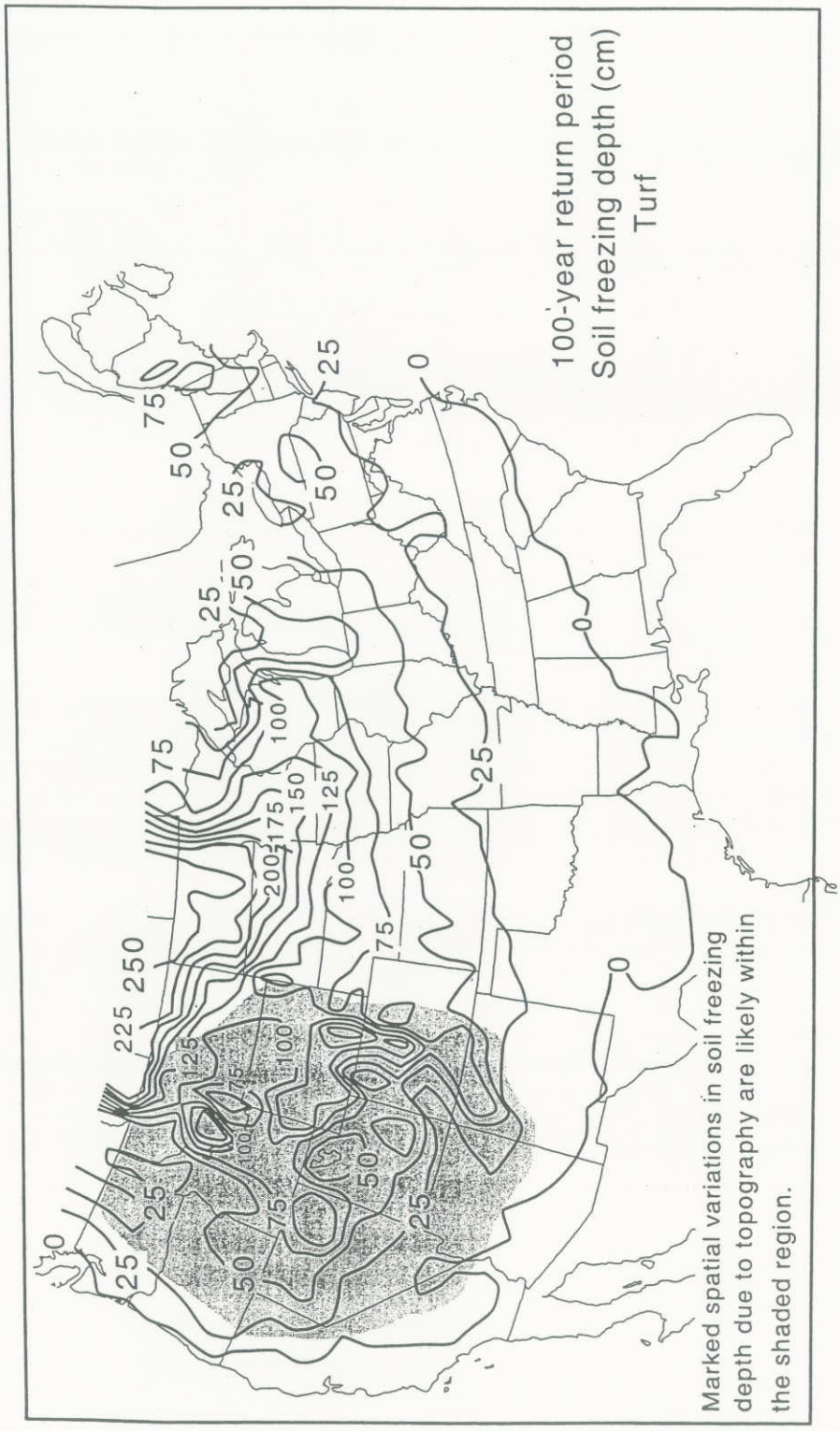
100-year return period
Soil freezing depth (cm)
Turf
Marked spatial variations in soil freezing depth due to topography are likely within the shaded region.

International Residential Code **NOT SUBMITTED**
2003/2004 Code Development Cycle
Proponent: Dick Morris, NAHB
Prepared by: Jay Crandell, P.E.

Revise footnote 'b.' of Table R301.2(1) as follows:

b. The frost line depth may required deeper footings than indicated in Figure R403.1(1). The jurisdiction shall fill in the frost line depth column with the minimum depth of footing below finish grade as determined in accordance with Section R403.1.4.

Revise Section R403.1.4.1 as follows:

R403.1.4 Minimum Depth. All exterior footings shall be placed at least 12 inches (305 mm) below the undisturbed ground. Where applicable, the depth of footings shall also conform to Section R403.1.4.1.

R403.1.4.1 Frost Protection. Except where otherwise protected from frost, foundation walls, piers and other permanent supports of buildings and structures shall be protected from frost by one or more of the following methods:

1. Extended below the frost line specified in Table R301.2(1) as determined using Table R403.1(2) and Figure R403.3(2).

(remainder of list unchanged)

Renumber Table R403.1 to R403.1(1) and change table reference in Section R403.1.1 accordingly.

Add a new Table R403.1(2) as follows:

TABLE R403.1(2)
FROST LINE DEPTH
(MINIMUM BOTTOM OF FOOTING DEPTH)

100-YEAR AIR-FREEZING INDEX [Figure R403.3(2)]	FROST LINE DEPTH (inches)
≤ 350	12
500	16
1000	24
1500	32
2000	40
2500	45
3000	52
3500	57
4000	62
4250	65

SUBSTANTIATION: New climate studies, frost-depth data, and risk modeling efforts have improved the understanding of variation in normal and extreme frost depths in the United States. These studies have been conducted by the National Oceanic and Atmospheric Administration and the NOAA Northeast Regional Climate Center at Cornell University under the sponsorship of the U.S. Department of Housing and Urban Development and the National Association of Home Builders. Current methods of establishing local frost line depths are generally consistent with trends in the newer data, but are often in disagreement with frost penetration data, variations in frost depth based on the Air-freezing Index, and results of updated climatic risk models. This proposal calibrates the results of this newer data to closely match current design frost line depths used in the colder U.S. climates and correlates these depths to the air-freezing index in a risk-consistent manner to improve current practice throughout the United States. The approach is equivalent to using an average frost penetration depth for bare soil multiplied by a safety factor of 2 as illustrated in the following graph:

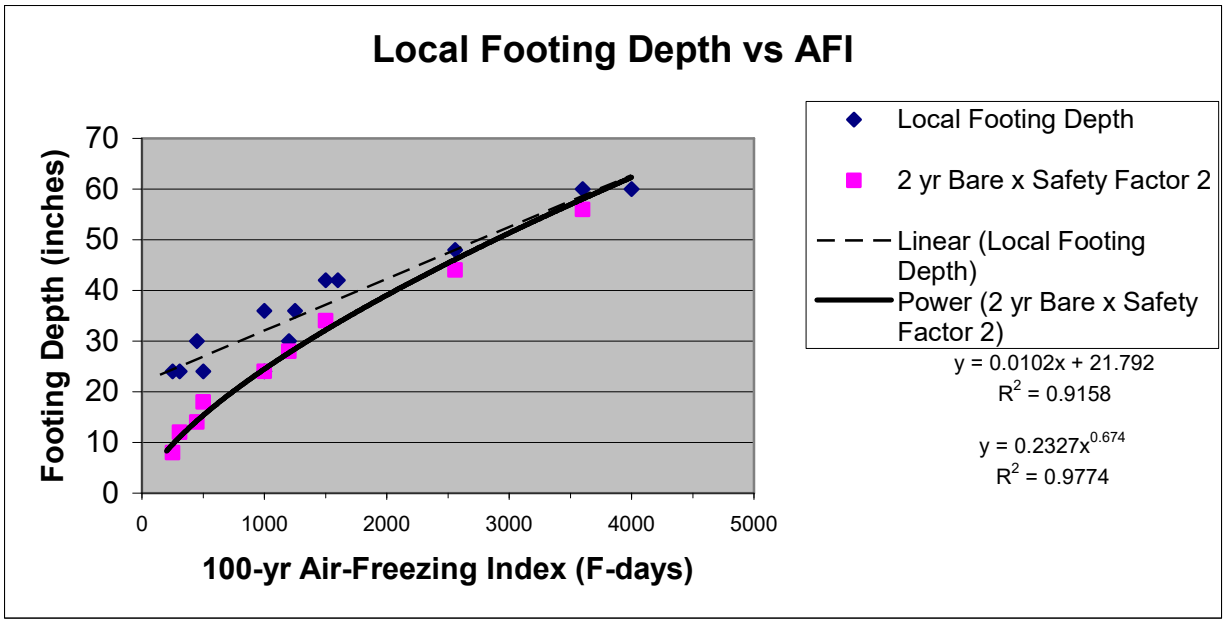

The frost depths determined using the above approach do not explicitly account for the effect that occupied buildings (i.e., heated buildings) have on the frost line depth. In some jurisdictions footing depths for "warm" foundations are decreased from that shown in the chart above. For example, the depth for a residential building foundation is reduced from 60 inches to 42 inches in Palmer, Alaska and Anchorage, Alaska. This is done along with the practice of requiring a minimum R10 insulation on the foundation wall which is similar to the frost protection requirements found in the ASCE 32-01 standard referenced in Section R403.4.1 of the IRC and the frost protected shallow foundation requirements in Section R403.3 of the IRC. Thus, greater consistency in frost protection requirements across various accepted frost-protection methods is also achieved by this proposal.

References:

Development of Frost Depth Maps for the United States, U.S. Department of Housing and Urban Development, Washington, DC. July 2001.

Steuer, P.M. Methods Used to Create an Estimate of the 100-Year Return Period of the Air-Freezing Index, U.S. Department of Commerce, National Oceanic and Atmospheric Administration, National Climatic Data Center, Asheville, NC (1989).

Steuer, P.M. and J.H. Crandell. Comparison of Methods Used to Create an Estimate of the Air-Freezing Index, Journal of Cold Regions Engineering, 9:2. American Society of Civil Engineers, Reston, VA. June 1995.

ASCE Standard 32-01 Design and Construction of Frost-Protected Shallow Foundations, American Society of Civil Engineers, Reston, VA. 2001.

Crandell, J.H., Survey of Frost Line Depths Used by Local Building Departments in the U.S., Applied Residential Engineering Services, West River, MD. (unpublished data).

Average Annual Frost Penetration (Map), U.S. Department of Commerce, Weather Bureau (historic value)

Extreme Frost Penetration (Map), U.S. Department of Commerce, Weather Bureau (historic value and basis for some local frost depths).